University of Cyprus
Department of Civil and Environmental Engineering

AUTOGENOUS SHRINKAGE EFFECTS ON HIGH STRENGTH CONCRETE WITH MECHANICALLY TREATED AND INTERNALLY CURED AGGREGATES

Charalambos Erotokritou, BSc Civil Engineer

Dissertation Paper

Nicosia, August 2023

Supervisor: Professor Dr. Michail F. Petrou
Professor at University of Cyprus at Civil and Environmental Engineers Department

DECLARATION

Unless noted otherwise, the work presented in this case study represents the original work of the author for the composition of this dissertation paper.

ACKNOWLEDGEMENT

The author of this case study would like to express gratitude towards the following individuals for their invaluable contribution to writing the case study/dissertation paper:

- **Dr Michael F. Petrou**: Professor at UCY and Supervisor of the research. His guidance and unwavering support were crucial in bringing this paper to completion.
- **Dr. Thomaida Polydorou and Dr. Demetris Demetriou**: PhD assistants to Dr. Michael F. Petrou. Their technical help and constructive feedback were extremely valuable through the whole research process.
- **PhD candidate Konstantina Oikonomopoulou**: For her assistance in locating standards and research papers, mixing formulation, specimen preparation, testing data acquisition and contributing to the writing of this case study.
- **M.Eng. students Alexandros Alexandrou & Neofytos Neofytou:** Their contribution in material preparation, specimen casting, test arrangement and data collection were integral to the success of this study.
- **Dr. Loukas Petrou and Mr. Michael Michael, UCY CEE lab staff:** Their expertise in assembling equipment and experimental test conditions facilitated the testing phase of this research.

The collaborative contributions of the aforementioned individuals have been extremely important in successfully concluding this dissertation paper.

Contents

List of Tables

List of Figures

ABBREVIATIONS

AD	Air Dried
CA	Coarse Aggregates
CS	Compressive Strength
FA	Fine Aggregates

FI	Flakiness Index
FS	Flexural Strength
NA	Natural Aggregates
OD	Oven Dried
SI	Shape Index
SP	Superplasticizer
SSD	Saturated Surface Dry
NC	Normal Aggregate Concrete
RFC	Recycled Field Aggregate Concrete
RTC	Recycled Treated Aggregate Concrete
RICTC	Recycled Internal Cured Treated Aggregate Concrete
RCA	Recycled Concrete Aggregates
RAC	Recycled Aggregate Concrete

ABSTRACT

The growing urgency to preserve natural resources has spurred the adoption of recycled concrete aggregates (RCA) in the production of conventional concrete. However, a significant drawback of recycled aggregate concrete (RAC) lies in the presence of hardened paste surrounding the aggregates resulting in an overall decrease in the material properties. To address this concern, various techniques for treating RCA have been employed to remove the adhered mortar partially or fully from the RCA's surface, aiming to enhance mechanical and durability properties. Additionally, internal curing of RCA has been investigated to enhance mechanical and durability properties.

This study employs ASTM C1581 and EN 12390-16 standards to evaluate shrinkage, specifically autogenous and drying shrinkage, and investigates the correlation between these tests. Furthermore, this study explores the impact of RCA on mechanical and durability experimental tests such as compressive strength, porosity, sorptivity etc.

The findings demonstrate that internal curing of treated RCA effectively reduces drying and autogenous shrinkage, reducing the risk of cracks. This positive outcome is mainly attributed to the internal hydration of cement from the saturated surface dry condition of the aggregates, also enhancing overall properties of RAC,

Finally, an innovative testing apparatus for large-scale autogenous shrinkage testing is proposed based on ASTM C1698. This new approach offers a promising pathway for accessing concrete's autogenous shrinkage and advancing our comprehension of RAC's performance.

1. Introduction

1.1 Concrete's influence on Economy, Society and Environment

Concrete is widely recognized as one of the most prevalent building materials, alongside steel and wood, with a history dating back to 6500 B.C. Archaeological findings indicate that similar materials resembling concrete, were utilized by ancient civilizations such as the Romans, Egyptians, and Chinese [1]. This composite material comprises fine, and coarse aggregates bound together with cement, which gradually hardens through hydration when water is added [2].

The impact of concrete production on the economy, society, and the natural environment has far-reaching implications. As mentioned earlier, concrete stands as one of the most widely used materials globally. Therefore, any positive or negative changes have significant consequences on the economy, while simultaneously affecting society and the natural surroundings. Unfortunately, the uncontrolled use of concrete has led many nations, including Cyprus, to cause severe damage to their natural environments, sometimes to an almost irreversible extent.

The process of extracting aggregates and producing cement requires a substantial amount of energy and fuel. For instance, as presented in Table 1, in the United Kingdom, the electricity consumption for producing 105.5 million tons of aggregate in 2009 reached 1,235,500 MWh [6], equivalent to a quarter of Cyprus's total electricity usage in the same year (Table 2) [7]. Furthermore, the emissions released during concrete production contribute to atmospheric pollution, harming the ozone layer and negatively impacting overall air quality [8].

In Cyprus, the annual production of aggregates for the years 2018 and 2019 is illustrated in table 2. Notably, there has been a 5.5% increase in aggregate production, indicating that the demands of the building industry continue to rise.

These findings emphasize the urgent need for sustainable practices and responsible management in concrete production to mitigate the adverse effects on the economy, society, and the natural environment. By implementing environmentally friendly measures and exploring innovative solutions, the concrete industry can play a significant role in promoting a more sustainable future.

Table 1: UK annual production of aggregates, consumption of energy and CO2 emissions [6].

	2009
Total Production (million tons)	105.50
Total Energy Consumption (MWh)	1,235,500
Crushed Rock Average SEC (kWh/ton)	14.20
Total $C0_2$ Emissions (tons)	430,000
Crushed Rock Average SCE ($kgC0_2$ / Ton)	4.60

Table 2: Electricity consumption and production for 2019 total and per capita [7].

Electricity	**Total**	**Cyprus Per Capita**
Own Consumption	4.36 bn kWh	3,582,63 kWh
Production	4.62 bn kWh	3,798,98 kWh

Table 3: Cyprus annual production of aggregates for 2018, 2019 [32].

	2018	2019
Total Production (million tons)	7.60	8.42

1.2 Recycled Aggregate Concrete Constituents

1.2.1 Cement 52.5 from Vasiliko cement plant

A hydraulic material that hardens when mixed with water, cement is composed of burnt calcite lime and clay. Lime is taken from limestone and chalk, while clay and slate is taken from the very same materials name. It serves as the primary component for mortars and concrete [4]. One of the most well-known types of cement worldwide is Portland cement, which was invented by Joseph Apsdin in 1824. The major substances in cement are C_3S, C_2A, C_3A and C_4AF. When cement is hydrated, the following chemical reactions take place into the matrix:

For C_3S:

$$2(3CaO \cdot SiO_2) + 6H_2O \rightarrow 3CaO \cdot 2SiO_2 \cdot 3H_2O + 3Ca(OH)_2$$

For C_2A:

$$2(2CaO \cdot SiO_2) + 4H_2O \rightarrow 3CaO \cdot 2SiO_2 \cdot 3H_2O + Ca(OH)_2$$

For C_3A:

$$3CaO \cdot Al_2O_3 + 6H_2O \rightarrow 3CaO \cdot Al_2O_3 \cdot 6H_2O$$

And for C_4AF:

$$4CaO \cdot Al_2O_3 \cdot Fe_2O_3 + 2Ca(OH)_2 + 10H_2O \rightarrow 3CaO \cdot Al_2O_3 \cdot 6H_2O + 3CaO \cdot Fe_2O_3 \cdot 6H_2O$$

The chemical reaction of the equations is exothermic. C_3A is the most exothermic substance in cement. Depending on the percentage of each element in the cement, the properties of the hardened product will differ. For example, cement with high concentrations of C_3A and For C_3A will increase the temperature of concrete which will result in cracking [48].

In this study, Type 52.5N cement from a Vasiliko cement factory was used.

1.2.2 Water

Being the most abundant substance on Earth and one of the most extensively utilized resources in the construction industry, water plays an indispensable role in the hydration of cement. Only clean water, free from sulfuric or chloride substances, is deemed suitable for use in concrete [5], as these impurities can have detrimental effects on its physical and mechanical properties.

1.2.3 Aggregates

These particles are used in producing employed compacted materials and are obtained by crushing rocks into smaller particles, which are then utilized in concrete manufacturing [3]. Aggregates can vary in size, type, and physical and mechanical properties, depending on the intended concrete

application. Some aggregates may be porous or contaminated by chloride (CL) or sulfuric substances. In Cyprus, the most prevalent aggregate type is diabase, sourced from quarries situated on mountainous terraces. Additionally, limestone aggregates are extracted from the Mitsero quarry.

1.2.4 Recycled concrete aggregates (RCA)

RCA are derived from construction and demolition waste materials (CDW), which are crushed to create different aggregate classifications. These materials are considered self-sustaining because they repurpose what was once considered useless into building materials. This approach reduces the need for natural resource extraction from quarries making it an environmentally friendly choice. Additionally, this process is defined as energy-efficient, since demolished buildings provide a readily available source, minimized the need for employing extensive quarry machinery [22].

Despite the environmental benefits, the incorporation of RCA in conventional concrete is well-known to reduce RAC's overall properties for two main reasons. Firstly, the aggregates undergo damage during the crushing process, leading to alterations in shape and pore structures that negatively affect concrete properties. For instance, flatter aggregates reduce concrete's compressive strength since, under pressure, these aggregates can shift, causing the composite to crack more readily [23]. Secondly, RCA is coated with cement paste, negatively affecting the mechanical and durability properties of RAC. Cement paste exhibits higher porosity compared to aggregates, resulting in higher porosity within RAC and, therefore, decreasing compressive and flexural strength, as these pores contribute to cracking mechanisms [9].

The effect of the adhered mortar on RCA has been extensively studied by numerous scientists as summarized below:

Table 4: Work from various researchers about recycled aggregates.

Author	Title	Goal of study	Results
Konstantina Oikonomopoulou et al.	Effect of Mechanically Treated Recycled Aggregates on the Long Term Mechanical Properties and Durability of Concrete [15]	The effects of an optimal mechanical treatment method to reduce the mortar adhered on recycled aggregates (RCA) on the long-term mechanical properties and durability of concretes containing RCA at different replacement levels.	Strain and mass loss are reduced, No threats from incorporation of treated or untreated aggregates in RAC.
P.Pliya	The compressive behavior of natural and recycled aggregate concrete during and after exposure to elevated temperatures [24]	Studying the performance of concrete made with RCA at elevated temperatures.	RCA exhibit satisfactory performance at elevated temperatures, which can be considered comparable to that of conventional concrete.

Eliane Khoury et al.	Impact of the initial moisture level and pre-wetting history of recycled concrete aggregates on their water absorption [25]	The influence of the initial moisture content and pre-wetting history of RCA on the properties of fresh recycled concrete, specifically slump.	The longer the RCA are wetted, the better the slump results.
Roumiana Zaharieva et al.	Frost resistance of recycled aggregate concrete [26]	Behavior of concrete with RCA in frosty environment	The higher porosity and lower mechanical characteristics of RAC render the concrete inadequately resistant to frost.
Assia Djerbi	Effect of recycled coarse aggregate on the new interfacial transition zone (ITZ) concrete [27]	Examine the influence of RCA on the microstructure of the new ITZ.	Generally, the reduction of water improves the porosity of the new ITZ.
Abdelaziz Hasnaoui et al.	Performance of metakaolin/slag-based geopolymer concrete made with recycled fine and coarse aggregates [28]	The potential utilization of both fine and coarse recycled demolition aggregates (RA) in the manufacturing of geopolymer concrete (GC).	The incorporation of RA into the mixes significantly adversely affects the mechanical properties.
Guanghao Yang et al.	Study on the Mechanical Properties and Durability of Recycled Aggregate Concrete under the Internal Curing Condition [29]	As shown in title	Utilizing pre-wetted RAC enhances the durability and mechanical properties of the concrete.
Peter Taylor et al.	Impacts of Internal Curing on Concrete Properties [30]	How IC influences the mechanical Properties of lightweight aggregates (LWA) for pavements	The warping of pavement slabs was minimized, leading to an increase in joint spacing overlays.

1.2.5 RCA adhered paste and Treatment Methods

As previously mentioned, the remnant mortar to the surface of RCA reduces the physio-mechanical properties of concrete. While certain studies were focused on partially removing the cement paste, Vivian W.Y. Tam attempted to fully remove the paste by employing acidic environments like HCl, H_3P0_4 and H_2SO_4 solutions, followed by water washing [11].

Figure 1: Aggregate paste removal procedure using acidic environment [11].

This technique effectively removes a significant portion or even the entire amount of the adhered mortar, thereby enhancing the physio-mechanical properties of the compound. However, it can have an adverse effect on the final product. The acidic environment alters the pH of the material. The essential high pH for concrete is crucial for the calcite that imparts the physio-mechanical properties. An acidic environment would degrade the calcite, leading to hardened concrete with reduced strength. Additionally, acids like HCl, H_3P0_4 and H_2SO_4 are notably expensive, dangerous and pose risks to both humans and the environment.

An alternative method to remove the adhered paste is outlined in [33]. The aggregates underwent cycles of high heating (500 °C), followed by rapid cooling with water, until the paste was removed. Even though this procedure can remove the paste from the aggregates, it also poses potential harm. The composition of the aggregates should be considered. In the presence of gypsum-based aggregates, temperatures exceeding 40 °C can alter the gypsum bonding agent within them. Furthermore, high heat may damage the aggregates in another manner. Aggregates often retain some moisture even after thorough drying. Subjecting them to high heat can cause the water vapors to expand within the aggregate's cavities, creating internal pressure which may result in microcracks. This would lead to a loss of durability and strength in the final product.

The basis of this study is founded on an alternative treatment RCA method, which involves the partial removal of the remnant mortar. This method was investigated and presented in [12] and illustrated in Figure 2:

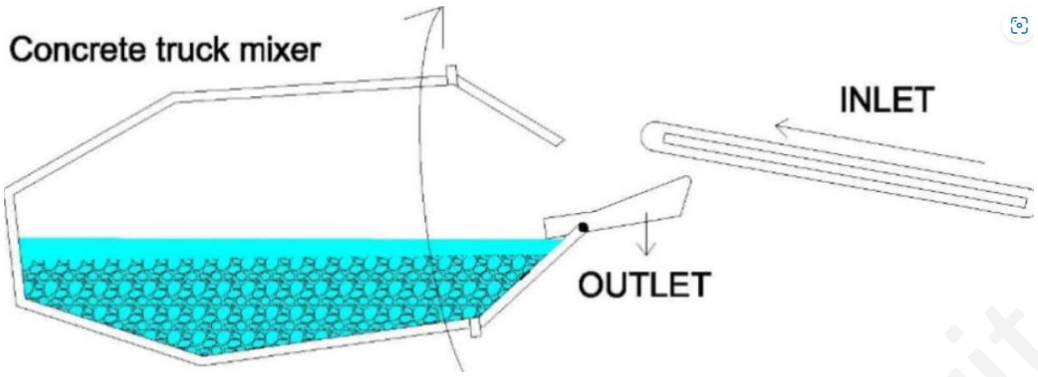

Figure 2: Low-cost removal of mortar paste from RCA [12].

The RCA were placed into a concrete truck mixture with equal amounts of water, and they were allowed to rotate for 3h colliding with the metal walls of the drums until a considerable degree of cement paste was removed. Afterwards, the aggregates were left with a sludge residue, which was subsequently rinsed with water.

This resulted in a higher strength and more durable concrete than the regular RCA concrete. It is stated in the paper that an increase of 25% of compressive strength was accumulated from 28 to 90 to 365 days by using different percentage of treated RAC each time. The shape of the aggregates was also affected, becoming rounder due to the cycling in the mixer. The treatment of aggregates helped also to reduce shrinkage to almost to 15% from reference concrete, reduced porosity to an extent depending on the aggregates replaced in the mix. The more treated aggregates into the mix, the less porosity was observed from treated aggregate mixes than the conventional recycled aggregates mixes. Lastly, studies showed that use of untreated or untreated in the mixtures will not need to have any durability concerns. These findings are considered to further help the use of RAC in the building industry.

1.3 Internal curing

Internal curing is a process involving the addition of pre-wetted aggregates to the concrete mix. As cement is a hydraulic material that requires water to undergo the reaction process, proper hydration is crucial. Unfortunately, even with thorough mixing, certain cement particles may not hydrate effectively. These particles might absorb moisture from nearby aggregates or pores after hardening. Adding concrete's low permeability that restricts moisture penetration into the matrix, the anhydrate clinker tends to concentrate on the available surrounding moisture. As a result, the excess free water within the pores gets absorbed, creating voids within the ITZ (interfacial transition zone). This leads to the development of internal stress, eventually culminating in the formation of micro cracks within the matrix [35].

By incorporating pre-wetted aggregates, a more efficient hydration of anhydrate cement particles is ensured. This approach effectively minimized the occurrence of cracks in the matrix, thus enhancing mechanical properties and durability.

2. Methodology

2.1 Testing on aggregates

For the characterization of the aggregates (4/10 mm, 0/4 mm and 0/2 mm) as well as the concrete samples, EN standards were employed. All utilized aggregates samples were collected based on EN 932-1:1996 and reduced in accordance with EN 932-2:1996, followed by oven-drying (OD) at a temperature of (110 ± 5° C) until a constant mass was achieved.

2.1.1 Particle Size Distribution

For the determination of particle size distribution of all implemented aggregates, the EN 933-1:2012 was applied. Samples that attainted constant mass were allowed to cool and then weighed. Afterwards, the samples were placed into a 0.063 mm sieve and thoroughly washed with water. Subsequently, they were oven-dried at a temperature of (110 ± 5° C) until a constant mass was achieved. Next, different sieve sizes (20, 14, 12, 10, 8, 6.3, 4, 2, 1, 0.063 and a pan) were arranged in descending order within the sieving column (Figure 3). The column was mechanically shaken for 10 minutes. The retained material on each sieve and in the pan was weighed.

Figure 3: Sieve machine used for the determination of the size distribution of aggregates.

The sieving method was used for RCA to achieve an identical particle size distribution as described in [15] and illustrated in Figure 17 found on Materials section under Aggregates

properties. This choice was made to facilitate easier evaluation of experimental results since the mixtures design remained consistent.

2.1.2 Water Absorption and Particle Density

The determination of particle density and water absorption of coarse aggregates was carried out in accordance with EN 1097-6:2013. For samples of 4/10 mm, particles passing the minimum and remaining on the maximum sieve were discarded after thorough washing. The remaining sample was then placed in a pyknometer filled with water at a temperature of (22 ± 3) °C. After ensuring the removal of entrapped air, the pyknometer was immersed in a water tank for (24 ± 0.5) h at a temperature of (22 ± 3) °C. Subsequently, another air removal step was performed, and the pyknometer, along with its cover, water and aggregate sample was weighted (M_2). The sample was then removed, and the pyknometer filled with water and covered was weighted (M_3). Temperatures were recorded before each session. Afterwards, the sample was placed in a dry cloth and gently patted until a state of saturated surfaced-dry (SSD) was achieved. The sample was then weighted (M_1). Finally, the sample was OD at a temperature of (110 ± 5° C) until a constant mass was achieved. After cooling, it was weighted (M_4).

Importantly, it should be noted that the fine aggregates utilized in this research were from the same batch used in [15], therefore the numerical results from that paper were applied for the mixtures design. Nonetheless, all experimental findings are presented in Chapter 3.1.1 Calculations of particle density and water absorption were executed based on the following formulations:

$$WA_{24} = \frac{100 \times (M_1 - M_4)}{M_4}$$

$$\rho_a = \rho_w \frac{M_4}{M_4 - (M_2 - M_3)}$$

$$\rho_{rd} = \rho_w \frac{M_4}{M_1 - (M_2 - M_3)}$$

$$\rho_{ssd} = \rho_w \frac{M_1}{M_1 - (M_2 - M_3)}$$

where
M_1: mass of the saturated surface-dried aggregate in the air, in grams
M_2: mass of the pyknometer containing the sample of saturated aggregate and water, in grams.
M_3: mass of the pyknometer filled with water only, in grams.
M_4: mass of the oven-dried test portion in air, in grams
WA_{24}: water absorption for 24 hr, in %
ρ_α: apparent particle density, in megagrams per cubic meter
ρ_{rd}: oven-dried particle density, in megagrams per cubic meter
ρ_{ssd}: saturated surface-dried particle density, in megagrams per cubic meter
ρ_w: density of water at the test temperature, in megagrams per cubic meter

2.1.3 Flakiness Index (FI)

The Flakiness index (FI), based on EN 933-3:2012 standard was employed to ascertain the thickness of coarse aggregates. The sample underwent an initial sieving process using a sieving machine to generate particle size fractions. Afterwards, all the segregated portions were weighed (particles passing through the smallest and those retained on the largest sieve being discarded). Subsequently, each of the separated fractions were individually subjected to manual sieved using bar sieves. These bar sieves were selected in accordance with Table 5 and were equipped with parallel slots as depicted in Figure 4).

Table 5: Circular sieves and bar sieves for Flakiness Index.

Size distribution sieve	Flakiness sieve
20/25	12.5 ± 0.4
16/20	10 ± 0.2
12.5/16	8 ± 0.2
10/12.5	6.3 ± 0.2
8/10	5 ± 0.2
6.3/8	4 ± 0.15
5/6.3	3.15 ± 0.15
4/5	2.5 ± 0.15

Figure 4: Flakiness index sieves.

The mass of the sample that passed the corresponding sieve was weighted. FI was calculated as presented in the following equation:

$$FI = \frac{M_2}{M_1} \times 100$$

where

M_1: sum of the masses of the particles in each of the particle size fraction, in grams

M_2: sum of the masses of the particles in each particle size fraction passing the corresponding bar sieve of slot width, in grams

2.1.4 Shape Index (SI)

The EN 933-4:2008 standard was employed to establish the shape index (SI) of 4/10 mm coarse aggregates. The initial sample was weighted (M_0) and then sieved as per the guidelines specified in EN 933-1:2012. Particles that remained on the largest sieve (25 mm) and particles that passed through the smallest sieve (4 mm) were discarded. Each segregated portion was weighed and if its mass was less than 10% of M_0, it was rejected. For each particle fraction, using a Vernier caliper all aggregates were manually measured for their length L (maximum dimension of a particle as defined by the greatest distance between two parallel planes tangential to the particle surface) and their thickness T (minimum dimension of a particle defined by the least distance between two parallel planes tangential to the particle surface). If the ratio L/T was greater than 3, the aggregate was categorized as non-cubical; conversely, if L/T was less than or equal to 3, it was categorized as cubical. The mass of non-cubical aggregates in each fraction was weighted, and subsequently, the SI was calculated using the following equation:

$$SI = \frac{M_2}{M_1} \times 100$$

where

M_1: mass of the test portion, in grams

M_2: mass of the non-cubical particles, in grams

2.2 Mixing, Casting and Curing

The study utilized mixtures previously outlined in [reference my paper]. These mixtures were characterized by a low w/c ratio of 0.25 (resulting in lower permeability compared to conventional concrete, thereby exacerbating autogenous shrinkage). The investigated mixtures as presented in Table 7 included the following combinations: a water-cured reference mixture without RCA (RC), a water-cured RAC mixture with 25% field RCA (RF), a water-cured RAC mixture with 25% treated RCA (RT) and an internally cured RAC formulation with treated RCA (RTIC).

Table 6: Mixtures that were investigated on this research based on [].

	Control (NC)	**Water Cured Recycled Field (RFC)**	**Water Cured Recycled Treated (RTC)**	**Internal Cured Recycled Treated (RICTC)**

CEM I 52.5N (kg/m^3)	864	864	864	864
Water (kg/m^3)	216	216	216	216
Coarse Natural 4/10 mm (kg/m^3)	730	548	547	547
Coarse Recycled 4/10 mm (kg/m^3)	0	183	182	182
Sand Diabase 0/4 mm (kg/m^3)	335	334	335	335
Latouros sand 0/2 (kg/m^3)	184	183	184	184
SP (%)	0.50	0.50	0.50	0.50
w/c ratio	0.25	0.25	0.25	0.25

To prepare the RTIC mixture, the RCA's were placed in a controlled environment of consistent temperature and humidity. They were soaked in predetermined quantities of water for a full day. The excess amounts of water along with the water absorbed from the aggregates were considered when determining the final mixing water volume.

The process was carried out in a 150L capacity pan mixer (Technotest). Initially, the coarse and fine aggregates were added, followed by incorporating half the portion of the water mix. This step was taken to minimize the dust generated from the cement and allowed the aggregated sufficient time to fill the surface voids with water. Subsequently, the cement was added and finally the remaining water along with the appropriate quantity of SP, was added to the mix. The concrete mixtures can be classified as Newtonian. They exhibited substantial workability initially, but after approximately 15 minutes, their workability rapidly diminished. The phenomenon can be attributed to the increased quantities of cement within the mixtures, causing rapid water absorption and consequently quick reduction in workability.

The casting of mixtures followed the guidelines outlined in BS 1881-125:2013 [21]. After casting, the samples were left to harden under damp cloths and reach a state suitable for demolding, which typically occurred around 24h after casting. Afterwards, samples were either water-cured in water tank at a temperature of (22 ± 3) °C or internally cured in air at a temperature of (25 ± 2) °C and relative humidity (RH) of (65 ± 5) % until the day of testing.

The table below (Table 8) presents the shapes of specimens, along with quantity of specimens for each experiment and the number of experimental repetitions:

Table 7: Experiments, Repetition, and samples for every experiment of the case study

Experiments	Day of experiment	Specimens	Size of Specimen (mm)
Compressive Strength EN 12390-3	1,3,7,28	3 cubes	100 x 100 x 100
Restrain Shrinkage ASTM1581	Every day until crack	1 ring	450 x 150 x 30
Modulus of Elasticity EN 12390-12	28	2 cylinders	150 x 300

Splitting Tensile Strength EN 12390-6	28	3 cylinders	100 x 200
Concrete Shrinkage EN 12390-16 (autogenous standard)	Every day for 28 days	2 prisms for drying, 2 for autogenous	75 x 75 x 280
Porosity [12390-7]	7, 28	4 cubes	100 x 100 x 100
Sorpivity [reference]	7,28	4 cubes	100 x 100 x 100

2.3 Testing on hardened concrete

2.3.1 Compressive and splitting tensile strength.

EN 12390-3 and EN 12390-6 standards were used to determine the compressive and splitting tensile strength, respectively. At the ages of 1, 3, 7 and 28 cubic specimens of 100 x 100 x 100 mm were tested in a 3000 kN capacity Technotest compression machine (Figure 6) with a loading rate of 0.6 ± 0.2 MPa/s. For splitting tensile strength determination cylindrical samples (100 mm x 200 m) were placed in a steel jig and tested in the Technotest compression machine with a loading rate of 0.05 ± 0.2 MPa/s. The following equation was used to evaluate the splitting tensile strength given from the computer.

$$f_{ct} = \frac{2 \times F}{\pi \times L \times d}$$

Where:

F: maximum load, in Newtons (N)

L: length of the line of contact of the specimen, in millimeters (mm)

d: designated cross-sectional dimension, in millimeters (mm)

Figure 5: Technotest compressive machinery for compression and splitting tensile tests.

2.3.2 Modulus of elasticity

The modulus of elasticity was determined by using a CONTROLS Advantest-9 hydraulic compression machine with a capacity of 5000KN (Figure 7). For each specimen, 3 strain gauges were attached at 120° to calculate the elasticity of concrete. The evaluation was conducted on the 28th day following concrete hardening, in accordance with the guidelines set by the standard EN 12390-13.

Figure 6: CONTROLS machine for EN 12390 -13.

2.3.3 Porosity & Sorpivity

For the determination of open porosity 4 cubic specimens were OD at a temperature of (70 ± 5° C) until a constant mass was achieved (m_d). Afterwards, all dried samples were placed in a vacuum vessel under a pressure of (2.0 ± 0.7) kPa for a duration of (2 ± 0.2) h. Subsequently, deionized water at temperature of (20 ± 5) °C was introduced and after complete immersion, the evacuation chamber was opened, allowing specimens to remain immersed for (24 ± 2) h. The mass of the specimens when fully immersed in water (m_h) and their mass in SSD condition (m_s) was weighted (Figure 8).

Figure 7: Setup for the determination of porosity of concrete.

The open porosity was calculated based on the following equation:

$$p_0 = \frac{m_s - m_d}{m_s - m_h} \times 100\ (\%)$$

To conduct the sorptivity test, four cubic specimens were employed. Initially, these cubes were OD until constant mass, which was then recorded (M_0). Subsequently, they were placed in glass containers to stabilize their temperature, preventing them from absorbing water vapors from the surrounding environment (Figure 9). For the experiment, propanol was added in circular disks. and plastic sticks were utilized to ensure that the edges of the cubes could effectively absorb the propanol. Weight data were collected at intervals of 1, 4, 9, 16, 25, 36, 49, 64 and 81 minutes. It is crucial to note that the measurements were taken at $t^{1/2}$ rather than t as indicated in the aforementioned equation in order to establish a linear relationship with the data.

$$\frac{Q}{A \times \rho} = k\sqrt{t}$$

Where:

Q is the amount of 2-Propanol absorbed, in gr

ρ is the density of propanol, in g/mm^3

A is the cross-section area that was exposed to propanol, in mm^2

t is the time of weighting, in min

k is the sorptivity coefficient, in $mm/s^{0.5}$

Figure 8: Setup for the sorptivity determination. The specimens were left into matrices until their temperature was stabilized.

2.3.4 Autogenous & Drying Shrinkage

Autogenous Shrinkage was assessed using the simplified method outlined in the standard procedure of EN12390-16 [43]. A total of four prisms each measuring 280mm X 75mm X 75mm were employed for the test. Out of these, two prisms were designated for drying shrinkage assessment and two were dedicated for the autogenous shrinkage determination. These specimens were stored in an environmental chamber with the specimens of ASTM 1581 with controlled humidity conditions. Over a span of 28 days following demolding, the shrinkage of the specimens was recorded daily. To ensure minimal moisture loss from the autogenous specimens, they were enclosed in aluminum duct tape. The following equations present the approach method employed by the author for calculating the shrinkage deformation of the specimens:

$$R = \frac{\sum(RE - S)}{n}$$

$$RF = R0 - R$$

where

R: resulting difference between reference bar and specimen for a specified day, whether was autogenous or drying in mm

Re: length of the reference bar, in mm

S: measurement from the specimen, in mm

n: number of specimens

RF: resulting shrinkage in mm

R0: first difference between the reference bar and the specimen.

By using these two equations, the author could calculate the total shrinkage of the specimen for a specified day from day 0.

Figure 9: Determination of drying (left) and autogenous (right) shrinkage.

2.3.5 ASTM 1698 & new novel setup

ASTM 1698, a relatively new procedure introduced by O. Mejlhede Jensen and P. Freiesleben Hansen in 1995 [13] serves to measure the linear autogenous shrinkage of mortars. This is carried out by using a specialized dilatometer as shown in Figure 11:

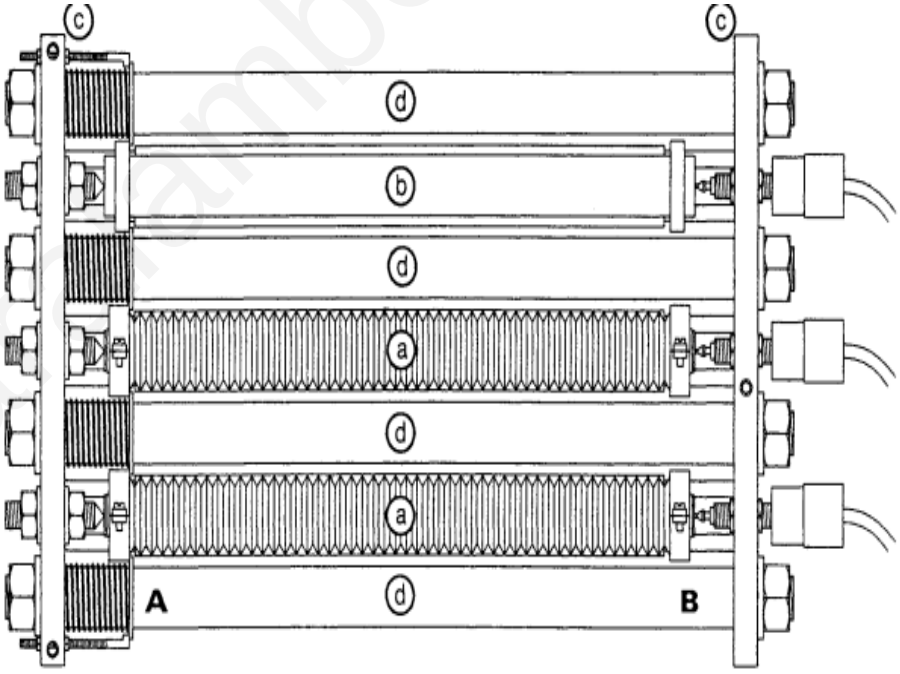

Figure 10:the original dilatometer as described by Mejihede.

The dilatometer includes a corrugated tube filled with mortar, inserted at its base. A LVDT attached at one edge measures the linear shrinkage of the tube while the opposite side remains fixed. However, measuring autogenous shrinkage is rather difficult, primarily due to the requirement to prevent moisture loss from the samples. In addition, high-precision equipment capable of measuring μm is essential. The intended procedure was initially designed solely to calculate the autogenous shrinkage of binders and mortar pastes. As such modifications to the setup were required to accommodate the size of the aggregates, which could potentially obstruct the filling of the tube or disrupt measurements due to blockage. To address this challenge, the dilatometer from ASTM1698 was custom-built at 2.5 times its original size as shown below:

Figure 11: Custom made dilatometer next to a dilatometer to its original size.

Both dilatometers were constructed from standard steel, a material susceptible to thermal deformation due to temperature fluctuations and also to oxidation when exposed to moisture To alleviate this issues, , the dilatometers were maintained within a controlled environment of consistent temperature and humidity during the tests and storage. To modify the autogenous shrinkage test procedure, specific adjustments were implemented for the specimens. Industrial plumping tubes were chosen as sampling tubes for sampling, as demonstrated below:

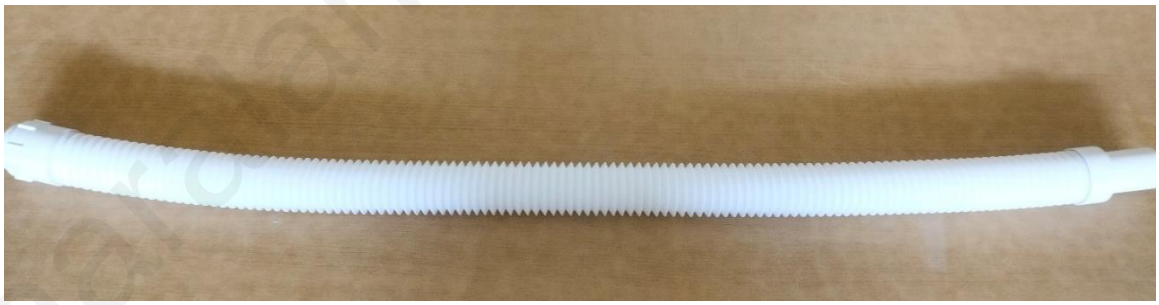

Figure 12: The tube for the specimens for ASTM 1698.

These tubes were corrugated with an internal diameter of 50 ± 0.5mm. During the process of filing the tubes at every one-third interval of the tube's length, it was placed on a vibrating table for 10 seconds. This contrasted with ASTM 1698's continuous vibration recommendation. This was due to the fact that ASTM 1698 applies to mortars and cement pastes. Continuous vibration in the case of concrete could lead to mixture's separation. Aside from this modification, all other aspects of the test adhered to ASTM 1698. Once the concrete was fully hardened, the edges of the tubes were trimmed to ensure a level surface for the LVDTs to make contact.

Several challenges emerged that required resolution prior initiating the test. The first involved the calibration of a strain transducer capable of precisely measuring 10mm of shrinkage with a precision of 0.0025mm. While numerous inexpensive transducers were available on the market, regular calibration was necessary imperative due to severe precision requirement for measuring shrinkage. The second challenge was to ensure the correct alignment of the reference bar with the transducer. To achieve this alignment, two plastic cylinders with central holes were introduced in conjunction with the reference bar. Ensuring the straightness of the tubes was the subsequent challenge in order to facilitate accurate shrinkage measurement. This was accomplished by inserting the tubes into 2 L-shaped steel corners with a length of 1m, effectively guaranteeing the straightness of the hardened concrete tubes.

Although there have been multiple calibrations and adjustments to the setup, it still remains in the experimentation phase. However, there is a belief that if everything goes as planned, the determination of autogenous shrinkage of concrete could be achieved soon. Below, you can see a cross-section and a transverse section of the specimen, illustrating the attempt to investigate this innovative setup:

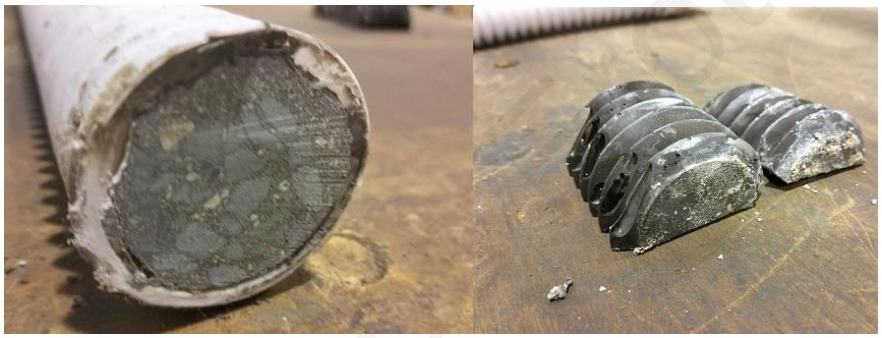

Figure 13: A section of the auto shrink specimen. The exposed concrete was covered with a water insulations substance that is used for roofs (left). The specimen from Figure 8. The specimen was cut in half to identify if the corrugations were successfully filled. The figure shows that more vibrations are needed to fully fill the corrugations (right).

2.3.6 Restraining Shrinkage

Also known as the ring test, this procedure test is thoroughly explained in ASTM 1581 standard. For the restraining shrinkage, one ring was molded for every mixture. The ring setup consists of an external ring with a diameter of 500mm, an internal ring with a diameter of 440mm, and a steel base, while the height was 150mm. In the literature, various sizes of ring have been used. The ring test has been extensively researched by numerous scientists in the last decade [36-41]. Initially, the rings were filled with concrete up to the midpoint. Using a steel rod, the rings were compacted as described in the ASTM standard. Following molding, the rings were placed in an environmental chamber to ensure consistent conditions during the curing process: :

Figure 14: The mold of the ring inside the environmental chamber.

After the concrete had hardened, the external ring and steel base were removed from the chamber. Three strain gauges were affixed to the rings at 120° intervals. The rings were then connected to a 3P strain gauge VISHAY indicator and recorder:

Figure 15: VISHAY 3P indicator and recorder. 4 strain gauges can be connected to measure the shrinkage in με.

Subsequently, the rings were left in the environmental chamber until cracking occurred. Data was collected at 15-minute intervals and an average of the data every 3h was recorded until cracking

was observed. The resulting graph depicting the cracking behavior of the rings is discussed in the following chapter.

3. Materials

All mixtures incorporated natural crushed diabase 4/10 coarse aggregates, diabase sand 0/4 mm and Latouros sand 0/2 mm. For the recycled mixtures, natural aggregates (NA) were replaced by 25% with recycled aggregates (RCA) both in their original state and after undergoing treatment. RCA's were sourced from a demolition site in Malunda village. While information regarding the building from which the RCA were obtained was unavailable, local residents mentioned that in the construction site the majority of the buildings stood in the village for over 40 years. In the case of treated aggregates, a 50L mixer was employed. The aggregates were placed in the mixer with the same quantity of water as that of the aggregates for a duration of 3h. After the 3h interval, the aggregates were sieved and subsequently allowed to dry for a day.

The primary binder for all mixtures was Portland Cement CEM I 52.5N from Vassilico Cement Works, with a specific gravity of 3.1 Mg/m^3 and its chemical composition is detailed in Table 6.

Table 8: Chemical Composition of CEM I 52.5N.

CaO (%)	**SiO_2 (%)**	**LOI (%)**	**AL_2O_3 (%)**	**SO_3 (%)**	**Fe_2O_3 (%)**	**MgO (%)**	**Alkalies (%)**
62.70	19.50	4.00	4.20	3.50	3.00	1.50	0.90

To enhance the workability of the mixtures due to low water-to-cement (w/c) ratio, a polycarboxylate superplasticizer (SP) was utilized. Ha-Be Pantrarhit 870, typically used at 0.2-2.0% of the cement weight, was employed to achieve the desired workability (S3 class). The mixing water was supplied by the laboratory and was free from chemicals and hazardous substances.

3.1 Aggregate Properties

3.1.1 Particle Size Distribution

Figure 17 illustrates the particle size distribution for the 4/10 mm normal coarse aggregates, as well as the field and treated 4/10 mm RCA. The aggregates followed the comprehensive procedures outlined in EN 933-1. Particle size distribution is considered among one of the most important tests conducted on aggregates prior to mixture formulation. By acknowledging the particle size distribution, one can assess the potential impact on workability and even the mechanical and physical attributes of the ensuing concrete. A distribution skewed towards larger particles tends to increase workability, although it may concurrently elevate porosity, possibly resulting in diminished strength. Conversely, a distribution closer to smaller particles could lead to less workable mixture, yet one characterized by reduced porosity, and consequently to increased strength and durability capabilities. The graph demonstrates that after treatment, the aggregated have a noticeable shift towards smaller particles in comparison to the RCA.

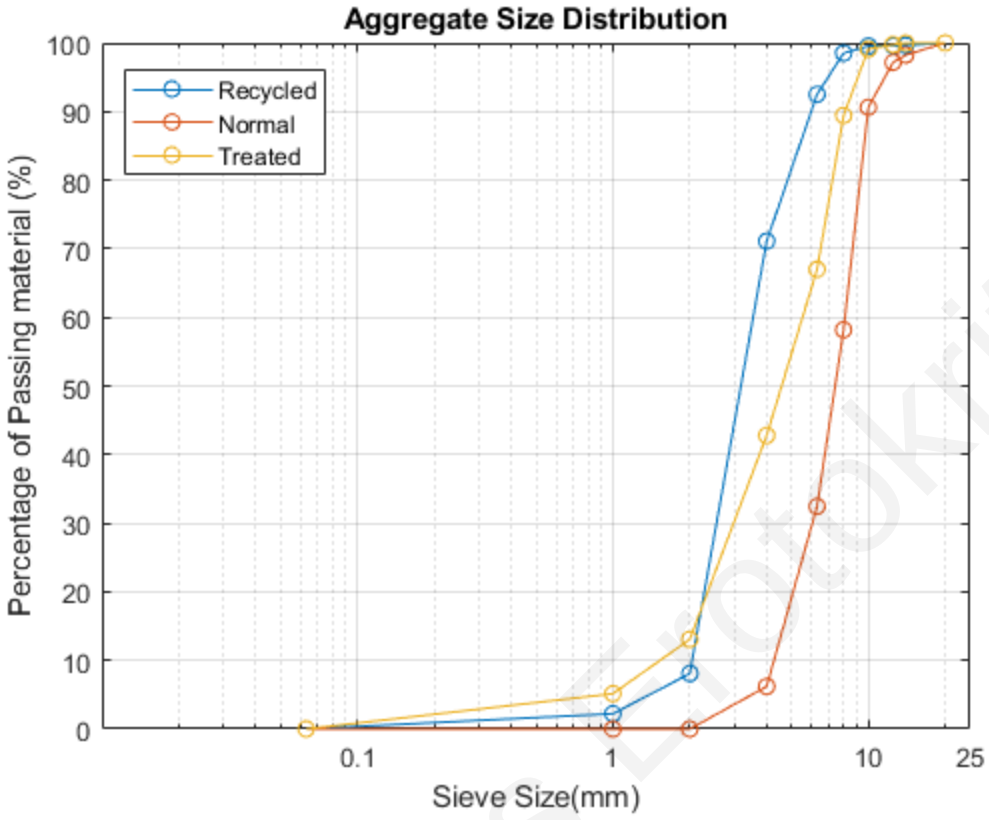

Figure 16: Particle size distribution of the 4/10 mm aggregates used in the case study [14].

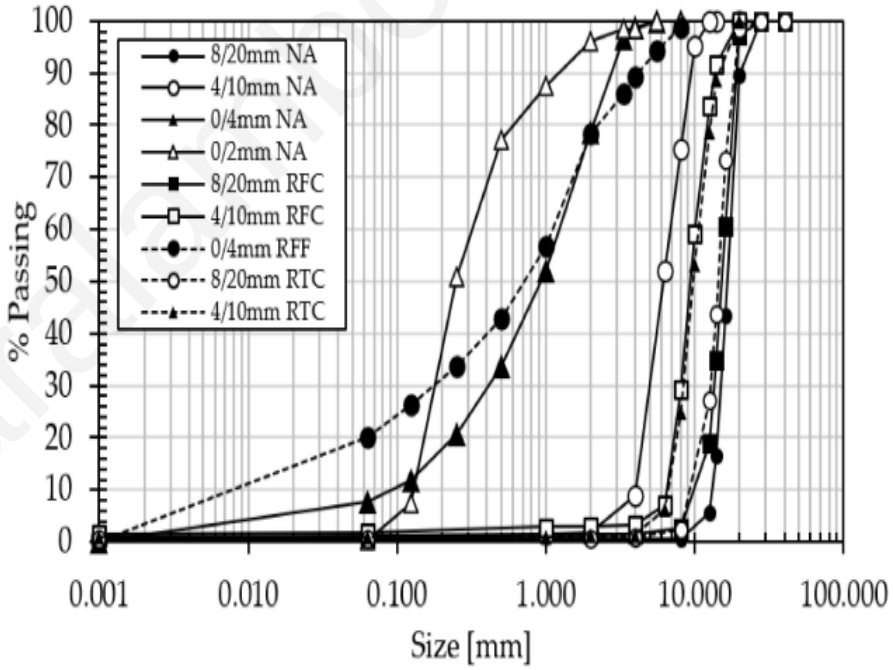

Figure 17: Size particle distribution as explained in Konstantina's case study about treated recycled aggregates [15].

3.1.2 Particle Density and Water Absorption

For the density of aggregates the results are shown in Table 9:

Table 9: Determination of apparent, saturated surface dry, immersed density and water absorption.

	4/10 mm Normal Aggregates	4/10 mm Recycled Field Aggregates	4/10 mm Recycled Treated Aggregates	0/4 mm Sand	0/2 mm Sand
p_a (kg/m^3)	2473	2665	2630	-	-
p_{rd} (kg/m^3)	2338	2371	2409	2267	2530
p_{ssd} (kg/m^3)	2392	2481	2493	2378	2580
WA_{24} (%)	2.34	4.64	3.48	4.89	1.8

3.1.3 Flakiness Index

The results (Tables 10-12) indicate that treated RCA exhibits a lower Flakiness index compared to field RCA. This reduction in FI is attributed to the presence of hardened paste around the aggregates. The removal of this paste led to an increase in the RCA's FI. However, a high FI is not always favorable for mixture design. Aggregates with high elongation might tend to slip under stress, as they are less likely to interlock with other aggregates in the matrix.

Table 10: Flakiness Index of 4/10 mm normal aggregates.

D size of sieve (mm)	Mass M_1 (gr)	Bar sieve (mm)	Mass M_2 (gr)
20	0.00	-	-
14	0.00	**12.5**	0.00
12.5	0.00	**10**	0.00
10	73.63	**8**	32.26
8	311.76	**6.3**	122.81
6.3	305.77	**5**	15.26
4	385.26	**4**	0.00
2	77.78	**3.15**	0.00
1	12.75	**2.5**	0.00
0.063	20.75	**2**	0.00
PAN	2.87	**-**	-
SUM M_1	1190.57	**SUM M_2**	170.33
FI	14		

Table 11: Flakiness Index of 4/10 mm field RCA.

D size of sieve (mm)	Mass M_1 (gr)	Bar sieve (mm)	Mass M_2 (gr)
20	0.00	-	-
14	77.07	**12.5**	14.36
12.5	203.07	**10**	0.00
10	2190.07	**8**	45.46
8	742.92	**6.3**	35.45
6.3	208.51	**5**	42.27
4	35.45	**4**	10.97
2	1.67	**3.15**	0.00
1	1.63	**2.5**	0.00
0.063	12.73	**2**	0.00
PAN	1.60	**-**	-
SUM M_1	3474.72	**SUM M_2**	148.51
FI	4		

Table 12: Flakiness Index of 4/10 mm treated RCA.

D size of sieve (mm)	Mass M_1 (gr)	Bar sieve (mm)	Mass M_2 (gr)
20	0.00	-	-
14	77.84	**12.5**	18.95
12.5	120.15	**10**	18.98
10	450.12	**8**	9.25
8	366.49	**6.3**	16.83
6.3	339.78	**5**	25.22
4	146.62	**4**	10.46
2	9.62	**3.15**	0.00
1	3.55	**2.5**	0.00
0.063	0.29	**2**	0.00
PAN	0.02	**-**	-
SUM M_1	1514.48	**SUM M_2**	99.69
FI	6		

3.1.4 Shape Index

The shape index results are presented in Tables 13-15. The findings indicate that aggregates of sieve size 6.3 to 10 are classified as square. According to existing literature [45], a higher shape

index signifies reduced workability in fresh concrete. However, it also suggests improved cohesion and a stronger matrix due to the enhanced of the internal locking between aggregates.

Table 13: Shape Index of 4/10 mm normal aggregates.

Sieve (mm)	Mass per sieve (g)	Mass of Square Aggregates (g)	Mass of Non-Square Aggregates (g)
>12.5	-	-	-
12.5	0	0	0
10	71.18	71.18	0
8	311.75	278.1	33.65
5	306.7	277.79	28.91
4	386.11	370.31	15.8
< 4	-	-	-
		M_2	78.36
M_1	1075.74	Total SI	8

Table 14: Shape Index of 4/10 mm field RCA.

Sieve (mm)	Mass per sieve (g)	Mass of Square Aggregates (g)	Mass of Non-Square Aggregates (g)
>12.5	-	-	-
12.5	203.07	0	0
10	2190.07	2051.23	138.84
8	742.92	704.22	38.7
5	208.51	0	0
4	35.45	0	0
< 4	-	-	-
SUM		M_2	177.15
M_1	3437.59	Total SI	6

Table 15: Shape Index of 4/10 mm treated RCA.

Sieve (mm)	Mass per sieve (g)	Mass of Square Aggregates (g)	Mass of Non-Square Aggregates (g)

>12.5	-	-	-
12.5	120.15	120.15	0
10	450.12	432.62	17.5
8	366.49	301.15	65.34
5	339.78	307.14	32.64
4	146.62	146.62	0
< 4	-	-	-
SUM		M_2	115.48
M_1	1303.01	Total SI	9

4. Experimental results & discussion

4.1 Hardened Concrete Properties

4.1.1 Compressive Strength

Compressive strength results were conducted in accordance with EN 12390-3, and the results are presented in Table 16:

Table 16: Test result from compression strength tests.

	NC	**RFC**	**RTC**	**RICTC**
7 day (MPa)	69.71	63.58	63.06	57.39
28 days (MPa)	70.72	64.40	66.13	58.53
Strength change (%)	1.47	1.27	4.64	1.94

As mentioned in Chapter 2 the four mixtures are categorized as follows: NC is a conventional concrete mixture with 0% RCA, RFC includes specimens from a mixture implementing 25% field 4/10 mm RCA, RTC denoted a water-cured mixture with treated RCA in the same ratio as RFC and RICTC is an internally cured mixture with 25% treated 4/10 mm RCA that were pre-soaked in water for 24h.

As anticipated the compression strength of NC was expected to be the highest at both 7 and 28 days. The least increase in compressive strength is observed in RFC specimens, while the most significant increase is seen in RTC specimens. This difference is attributed to the presence of paste adhered to the surface of RFC aggregates, leading to weaker matrix and faster cracking.

Among the specimens, RICTC specimens exhibited the lowest compression strength. Overall, an increase in compressive strength from 7 to 28 days was expected based on the results from [15] which formed the basis of the mix design. From the data in paper, a reduction in comparison between NC and RFC, RTC and RICTC show for the 7 days tests a percentage of 9.65%, 10.55% and 21.47% lower. Again for 28 days tests, NC is higher by a percentage of 8.93% for RFC, 6.94% for RTC and 20.82% for RICTC. From these data, it correlates that RTC showed the highest increase in compressive strength but also its capability was closer to NC than the rest. The problem that arises from this result is how RICTC, a mix which had the same type of aggregates with RTC and had internal curing treatment which is proven by literature to help increase the compressive strength of the samples, didn't met the expectations of the test.

This can be explained for the following reasons. Some specimens did not crack as expected due to buckling effect. Weaker areas on one side, caused by factors such as pores or previously present materials like glass and plastic in the aggregates, resulted in faster cracking and lower compressive strength. This unfortunately can't explain the lower strength of NC, since it was made from 100% natural aggregates. Another significant parameter affecting the test was consolidation, evident from the images (Figure 18) showing opening that could introduce weak spots in the concrete matrix leading to quicker cracking during the compression test. It was initially planned that the specimens would undergo vibration for a specific duration as reference in [15]. However, due to the hot climate, the mix hardened quickly, resulting in reduced workability. This in turn affected consolidation and led to the formation of small pores that impacted the strength during the compression test.

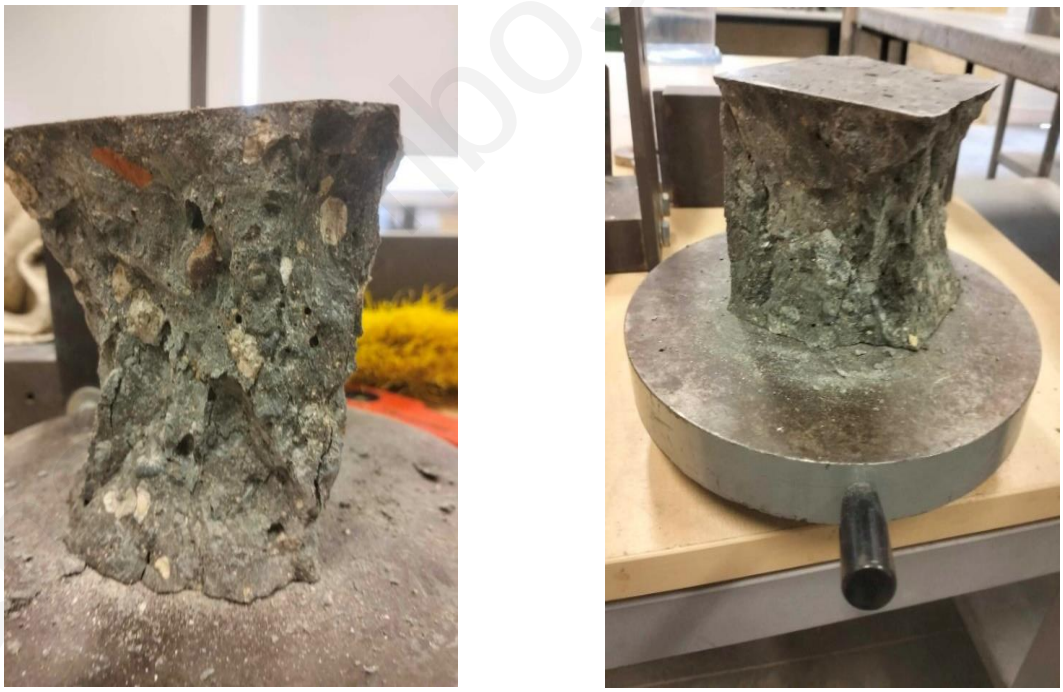

Figure 18: Test specimens after compression test. On the left, small holes and ceramic pieces, are shown which could affect the compression strength. On the right, the test specimen did not broke correctly due to buckling effect.

4.1.2 Splitting Tensile Strength

Splitting tensile strength results were conducted in accordance with EN 12390-6 and the results are presented in Table 17:

Table 17: Splitting tensile strength results for all investigated RAC mixtures.

	NC	RFC	RTC	RICTC
28 Days (MPa)	4.21	3.44	3.73	5.01

The test results indicate that RTIC exhibited the best performance in this test, primarily due to their high tensile strength failure mode. As expected, RF specimens once again displayed lower tensile strength, a consequence of the weaker matrix as previously discussed. The treatment of aggregates contributed to the increase in tensile strength, and the incorporation of internal curing further enhances the overall strength capabilities. The decrease of tensile strength in comparison to NC and RFC, RTC and RICTC is 18.29%, and -15.97%. From these results it shows that RICTC had a higher tensile strength than NC. Although it was expected that an increase in tensile strength was ensured due to internal curing treatment, it was not expected to be higher than NC.

Despite the observed increase in tensile strength following treatment, the results are still lower than what is typically reported in the literature. This could probably be attributed to the poor quality of aggregates and inadequate consolidation. The accelerated hardening process created voids, as previously noted, which led to the development of weaker areas within the concrete matrix. Additionally, the presence of hardened paste from the RCA further contributed to the reduction in tensile strength compared to anticipated values.

Figure 19: A specimen after the tensile failure. Some small opes can be identified inside the specimen which resulted into lower tensile strength than anticipated.

4.1.3 Modulus of Elasticity

Results from modulus of elasticity are demonstrated in Table18. Surprisingly, RFC specimens exhibited higher modulus of elasticity than RTC specimens by 2.15%. This outcome contradicted the initial expectations, as the presence of hardened paste in RFC mixture should theoretically lead to a weaker matrix, allowing for greater deformation. This phenomenon can be understood by considering the equation:

$$E = \frac{\sigma}{e}$$

Where E represents the modulus of elasticity strength, e is the strain and σ is the stress. According to this equation higher strain capacity would result in greater deformation and a lower modulus of elasticity. However, the use of internal curing in conjunction with the treatment method resulted into closing pores within the matrix, reducing its susceptibility to cracking. Consequently, both RFC and RTC specimens demonstrated higher modulus of elasticity due to this effect.

Table 18: Modulus of Elasticity for all RAC mixtures.

	NC	**RFC**	**RTC**	**RICTC**
28 Days (GPa)	28.25	23.25	22.75	26.25

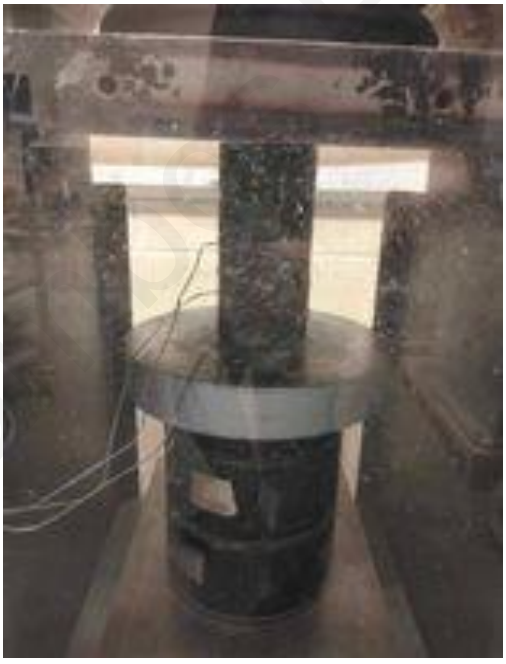

Figure 20: Setup of modulus of elasticity strength determination. 3 strain gauges were used in the middle of the cylinder at 120 degrees each.

4.1.4 Open Porosity & Sorptivity

Open porosity and sorptivity experiments were conducted following the guidelines outlined []. The obtained experimental results for open porosity are presented in Table 19:

Table 19: Open Porosity from 7 to 28 days for all RAC mixtures.

	NC (Control)	RFC (Recycled)	RTC (Treated)	RICTC (Water Cured/ Treated)
7 Days (%)	6.73	8.06	8.43	9.51
28 Days (%)	4.50	6.66	6.97	7.01

The results demonstrate that a reduction in porosity leads to an increase in compressive strength, which is consistent with existing literature. The treatment of aggregates contributed to the reduction of concrete porosity. This reduction is attributed to the removal of old cement paste from RCA, which can interfere with new cement paste adherence, and lead to a weaker Interfacial Transition Zone (ITZ) matrix than that of conventional concrete. By removing pre existing cement paste from RCA, better adherence with fresh cement paste is achieved and this phenomenon leads to fewer pores in the ITZ and a denser product overall. Figure 21 indicates that RTC mixture exhibits a larger strength increase than RICT. The difference can be attributed to the quality of the RCA utilized. The unpredicted nature of RCA's impact on RAC's mechanical capabilities and physical properties is evident. The greater the proportion of RCA in the mixture, the more pronounced its influence on the final product.

Furthermore, as expected, RFC is projected to show the smallest strength increase from 7 to 28 days, along with the lowest least increase in density. As before mentioned previously, it is greatly affected by the paste layer on the aggregates, which will result in creating a weaker ITZ matrix than the rest, which were treated to remove old cement paste. A weaker ITZ means more pores into the matrix and as aforementioned higher porosity, weaker adherence between aggregate and cement paste thus creating weak zones in the matrix and lead to lower mechanical capabilities.

Another result for discussion is that there is a greater decrease in porosity in the samples that were internally cured. Internal curing leads to producing more cement hydration products because water is released internally, reaching more anhydrate cement, and cement hydration continues for a longer period of time.

Figure 21 illustrated the correlation between porosity and compressive strength outcomes:

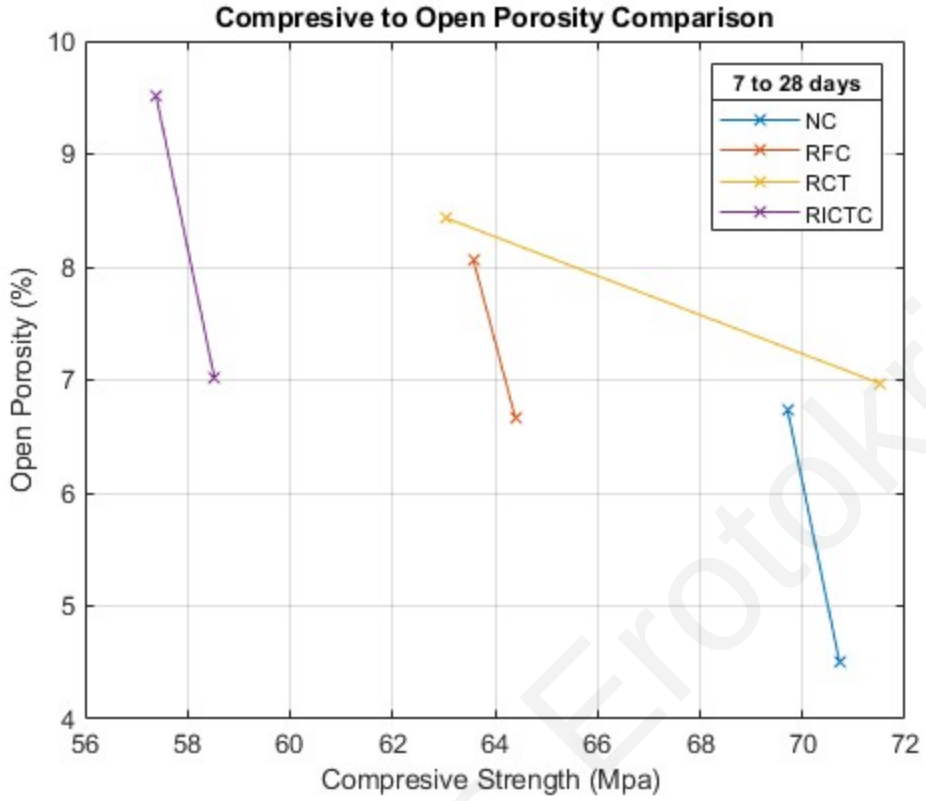

Figure 21: Correlation between Compressive strength and Porosity. The first bullet indicates 7 days tests and the second bullet 28 days results.

Figure 21 depicts the increase of compressive strength can be based in the decrease of the porosity. A mix with higher grade material will show a greater increase in strength like RTC than a mix with a lower grade material.

The sorptivity test results (Figures 22-25 and Table 20) demonstrate that RCT mixture exhibits steeper slope at 7 days compared to the other mixtures. A steeper slope indicates higher suction capacity of the material, which aligns with findings in the literature. At 28 days, the slopes decrease as expected, indicating that many pores have closed due to cement reactions, resulting in a denser material with reduced suction capabilities.

Consistent with literature, the lowest slope among all four mixtures is observed in RICTC concrete. The internal curing effectively moisturizes cement particles within the matrix, leading to the closure of. pores and reduced suction capabilities. Moreover, treatment also contributes to lowering the slope's steepness, enhancing the durability of the final product.

Table 20: Sorptivity coefficient for all RAC formulations.

	NC	**RFC**	**RTC**	**RICTC**
7 Days (mm/t$^{1/2}$)	0.0836	0.0814	0.087	0.0695
28 Days (mm/t$^{1/2}$)	0.0726	0.0737	0.0846	0.0662

As expected, all test results showed a decrease in sorpivity coefficient. RTC showed the lowest change from 7 to 28 days with a 2.75% percentage. RICTC also showed a small change to a percentage of 4.75%. It was expected that the biggest change would be from RFC due to the low material grade but instead it's from NC with a percentage of 13.16%.

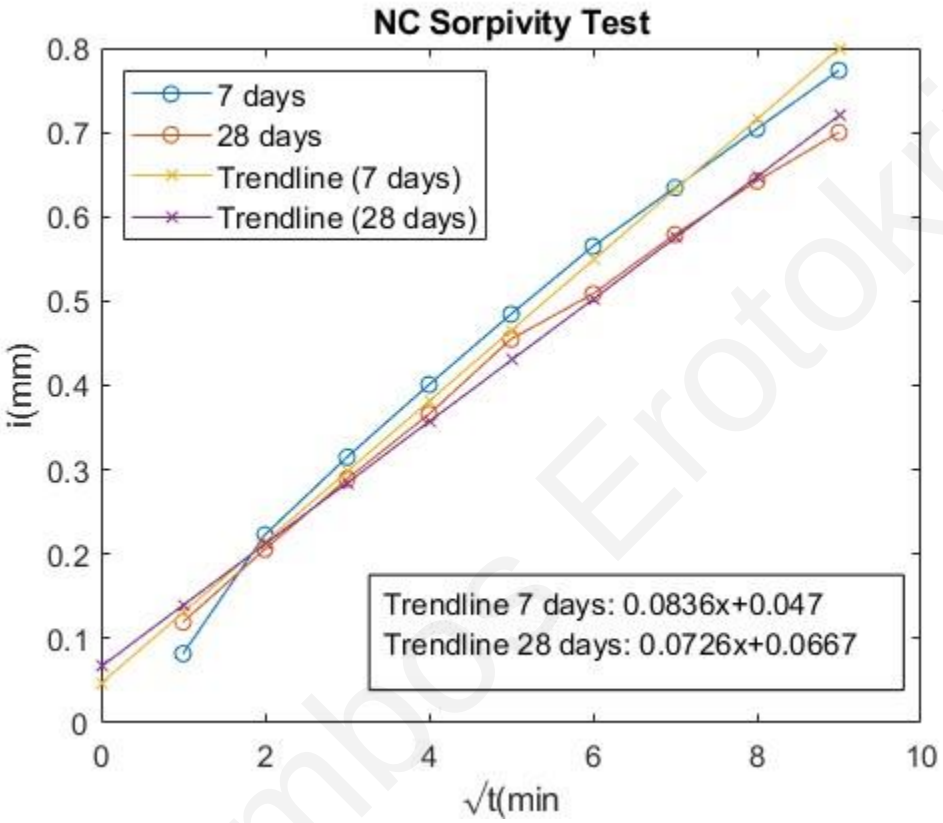

Figure 22: Sorptivity test results at 7 and 28 days for NC mixture. The upper equation is for 7 days and the lower for 28.

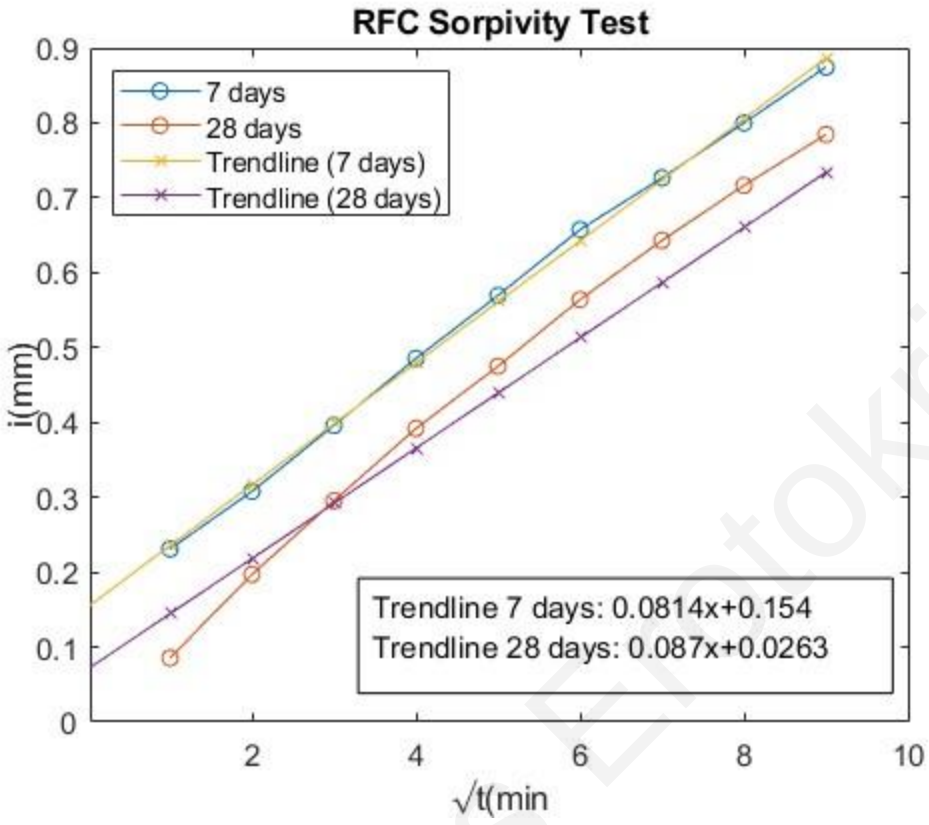

Figure 23: Sorptivity test results at 7 and 28 days for RFC mixture. The upper equation is for 7 days and the lower for 28.

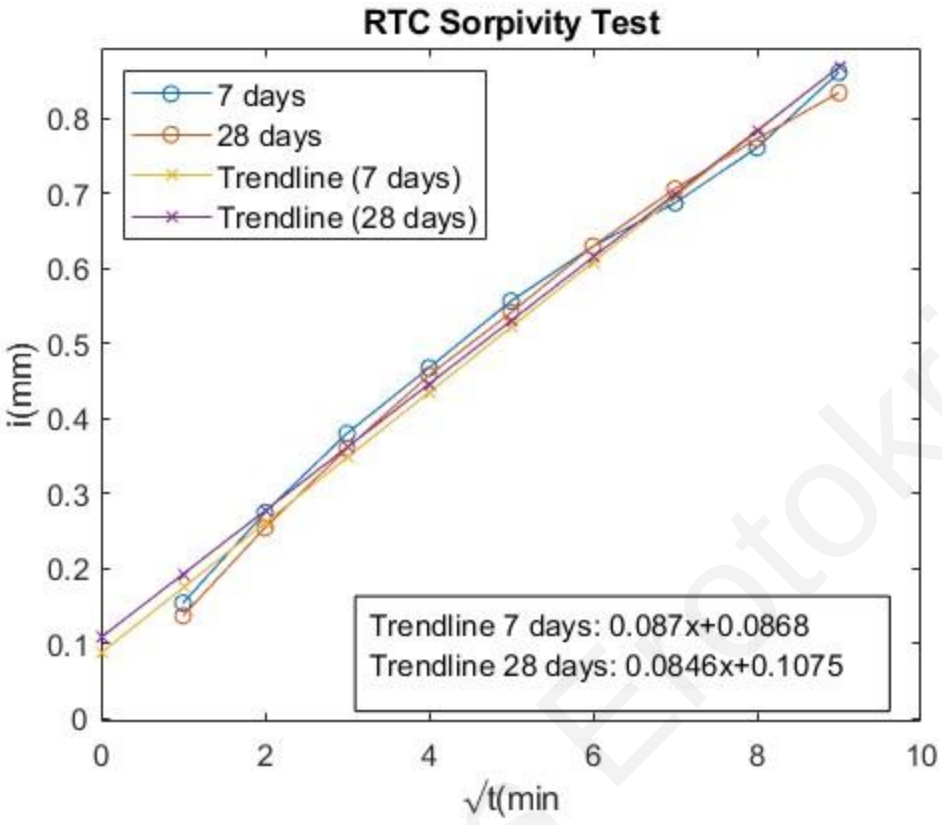

Figure 24: Sorptivity test results at 7 and 28 days for RTC mixture. The upper equation is for 7 days and the lower for 28.

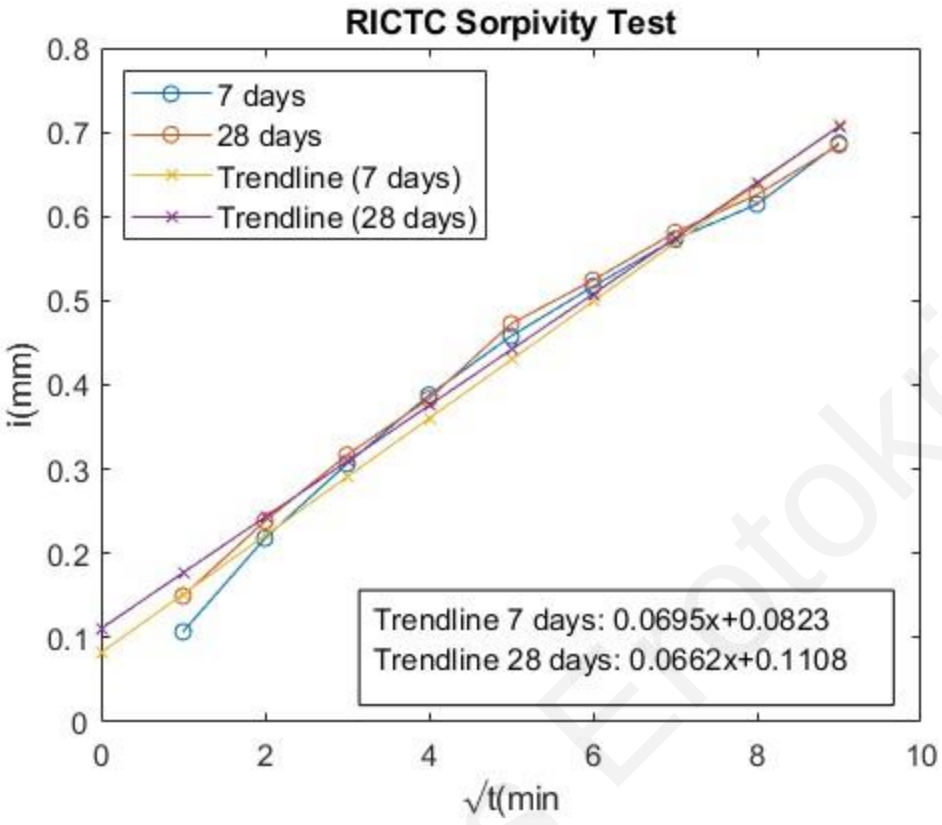

Figure 25: Sorptivity test results at 7 and 28 days for RICT mixture. The upper equation is for 7 days and the lower for 28.

4.1.5 Restrained Shrinkage

The experimental results for the restrained shrinkage test on all RAC mixtures are demonstrated in Figure 26. The observed outcomes diverge from the information available in the literature. In [49], the NC's mixtures ring test took 3 days rather than three-quarters of the time shown in this paper results. Furthermore, the restrained shrinkage reported in this research is 1.5 times greater than that found in [49]. Additionally, the ssd ring test, equivalent to internal curing in this study, took 8 days to fail, contrasting with the 1.5 days indicated in this paper.

Overall, this test's results exhibit significant deviations from the anticipated outcomes documented in existing literature. These disparities can be attributed to issues related to the handling of specimens within the environmental chamber, reaching approximately 30 °C with a tolerance of ±1 degree, which was then sustained at that level. The humidity levels remained relatively consistent at around 50% with a variance of ±3% maintained using water traps. Apart from these deviations, all other experimental parameters adhered to the guidelines outlined by ASTM 1581 (American Society for Testing and Materials).

The elevated temperature condition had the effect of causing external moisture on the specimens to evaporate. Consequently, the absence of moisture within the concrete allowed the inner, non-moisturized cement paste to absorb vapors from the surrounding environment. This unexpected phenomenon accelerated the development of micro-cracks at a faster rate than initially predicted.

Notably, the elevated temperature might have induced any residual water within the specimens to generate internal stresses due to vapor pressure. These accumulated stresses likely contributed to an acceleration in the cracking process, which was not in line with the originally anticipated outcomes.

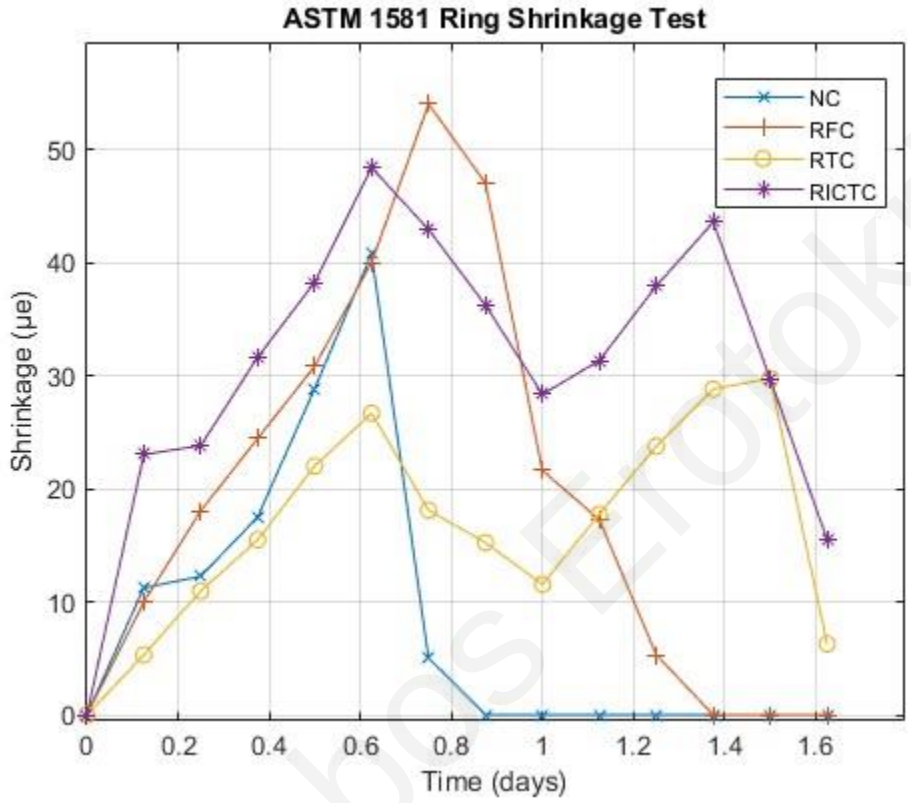

Figure 26: Shrinkage Test results for all mixtures based on ASTM 1581.

4.1.6 Drying Shrinkage & Autogenous Shrinkage

The following graphs (Figures 27-30) depict an initial period of heightened shrinkage rate, followed by a more stabilized trend. This indicates a significant reduction in the w/c reaction after the initial five-day period. As cement hydration progresses and the resulting products are smaller than the initial state, the shrinkage effect becomes less pronounced in the subsequent days. Regarding Autogenous shrinkage, specimens subjected to internal curing exhibit a more consistent rate. This can be attributed to the efficacy of the internal curing process in promoting cement hydration within the matrix, consequently reducing the occurrence of microcracking compared to other specimens.

In contrast, RTC autogenous shrinkage more closely aligns with the patterns observed in specimens treated with No Curing (NC) and Regular Curing (RFC). This highlights the significance of water content within the mixture. The utilization of wetted aggregates results in a more controlled state of autogenous shrinkage, thereby minimizing the potential for concrete cracking.

Moving on to Drying shrinkage, it is evident that RFC exhibits a higher rate compared to the other specimens. This can be attributed to the presence of hardened concrete paste, which adversely

affects the matrix. Existing cracks within the hardened paste facilitate the movement of vapors, prompting the cement to seek nearby water sources for hydration. This, in turn, accelerates the drying rate, generating internal stresses within the cement. As the cement absorbs water from its surroundings, this process is anticipated to result in a higher number of cracks compared to the other specimens.

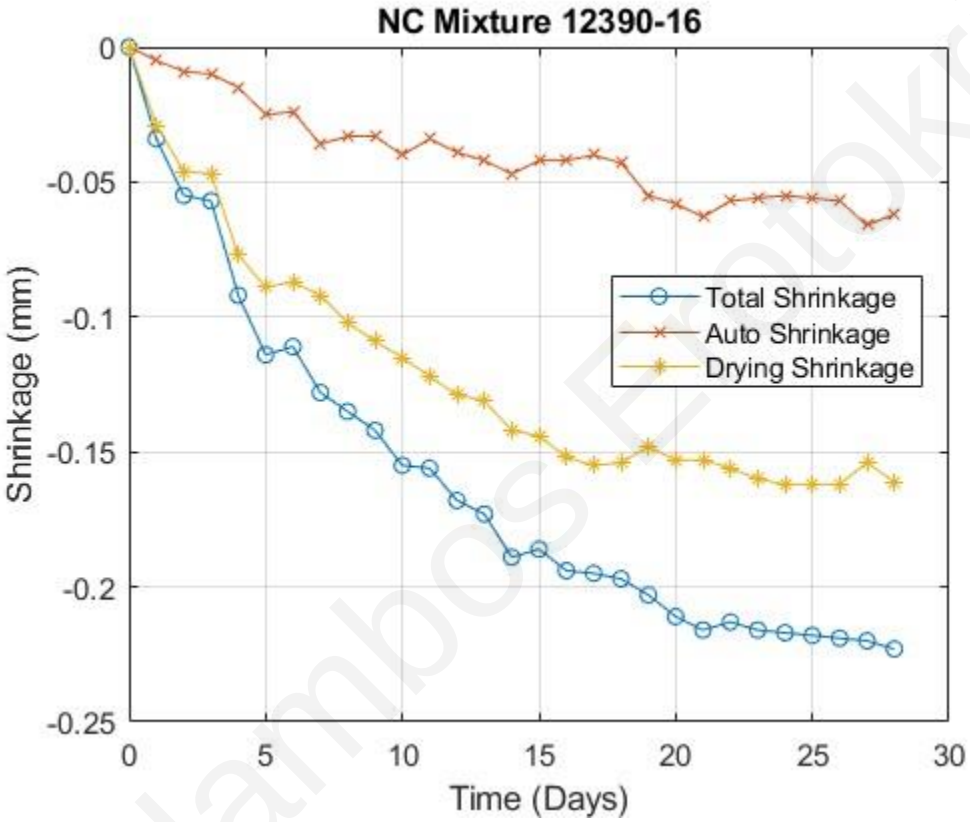

Figure 27: NC mixture total, autogenous and drying shrinkage results.

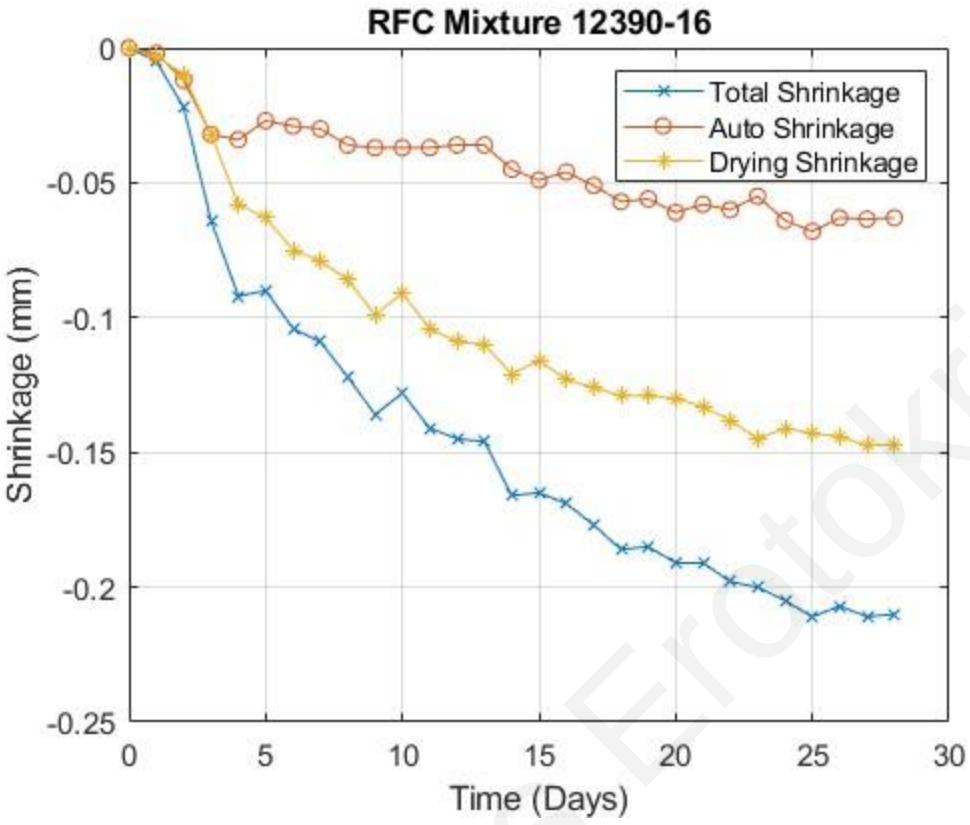

Figure 28: RFC mixture total, autogenous and drying shrinkage results.

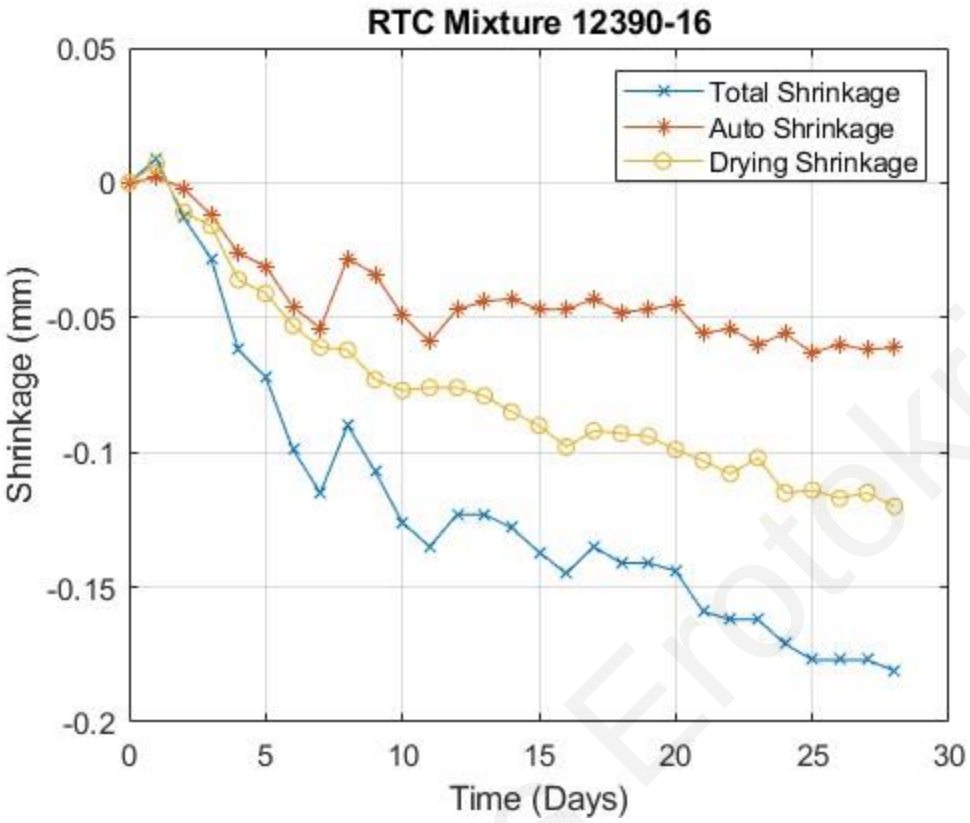

Figure 29: RTC mixture total, autogenous and drying shrinkage results.

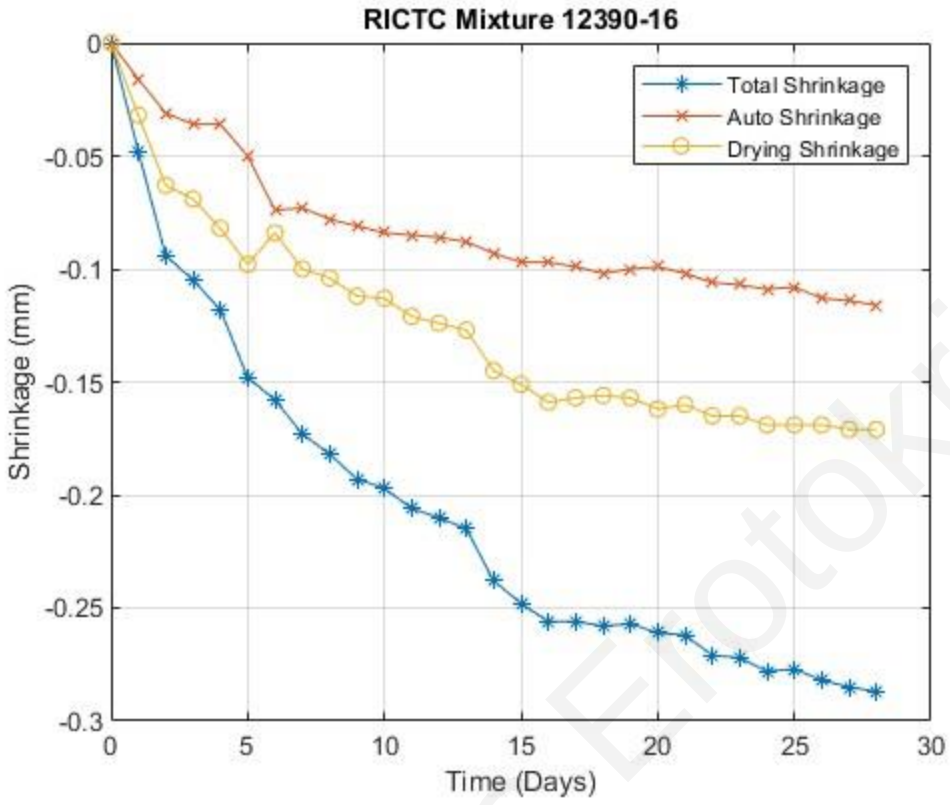

Figure 30: RICTC mixture total, autogenous and drying shrinkage results.

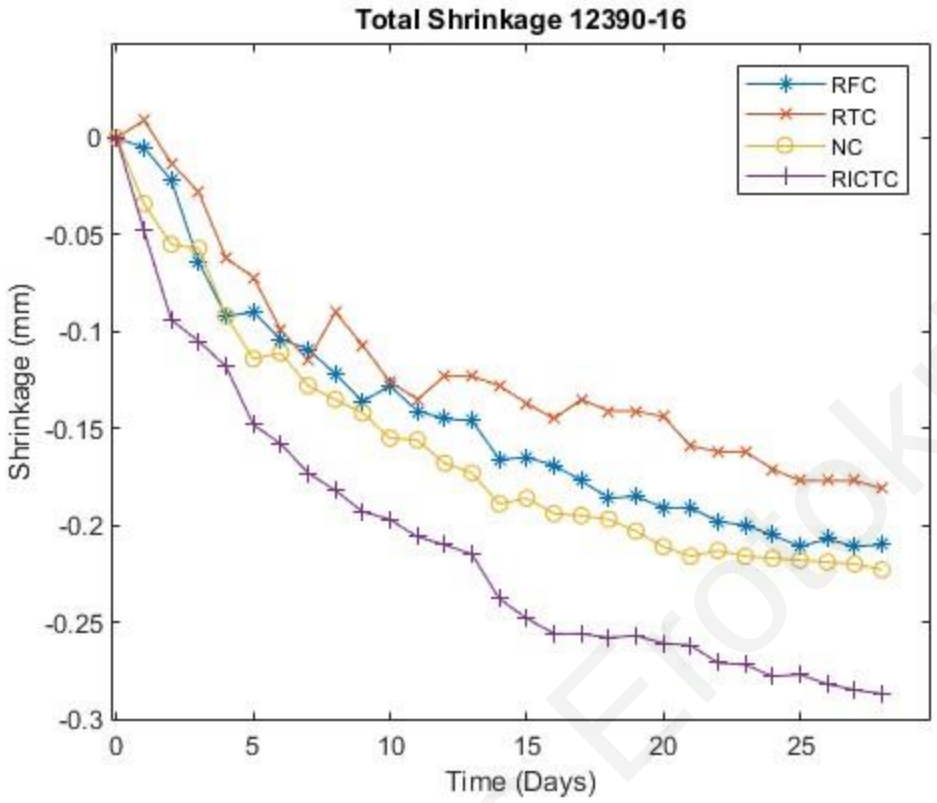

Figure 31 Total shrinkage of specimens versus time.

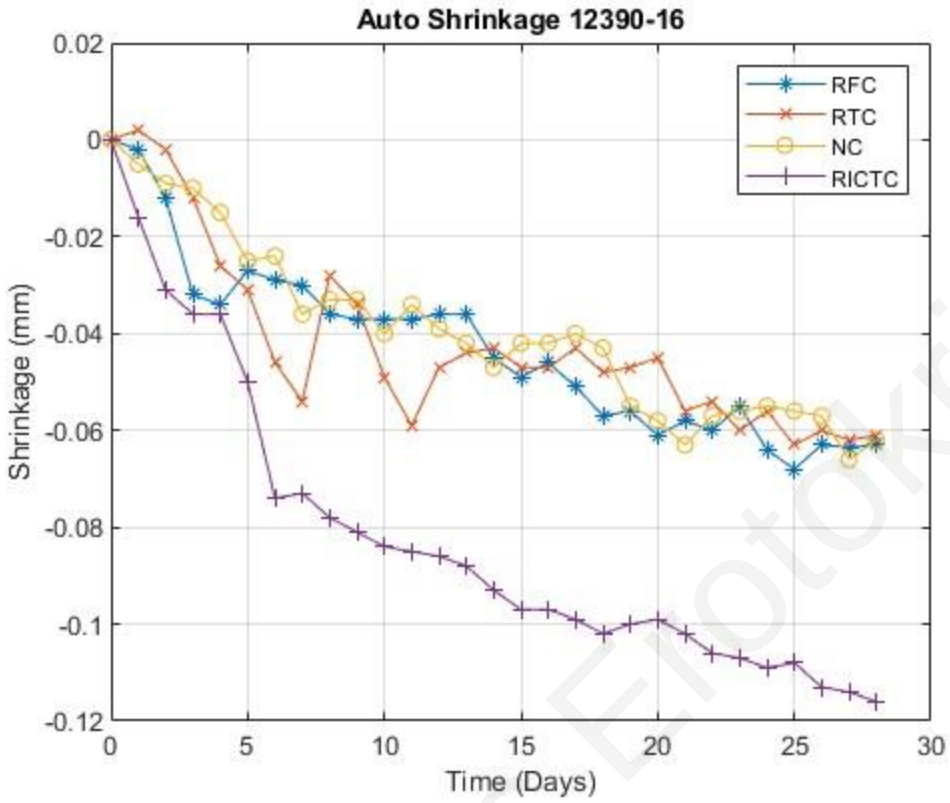

Figure 32 Total Auto Shrinkage of specimens versus time.

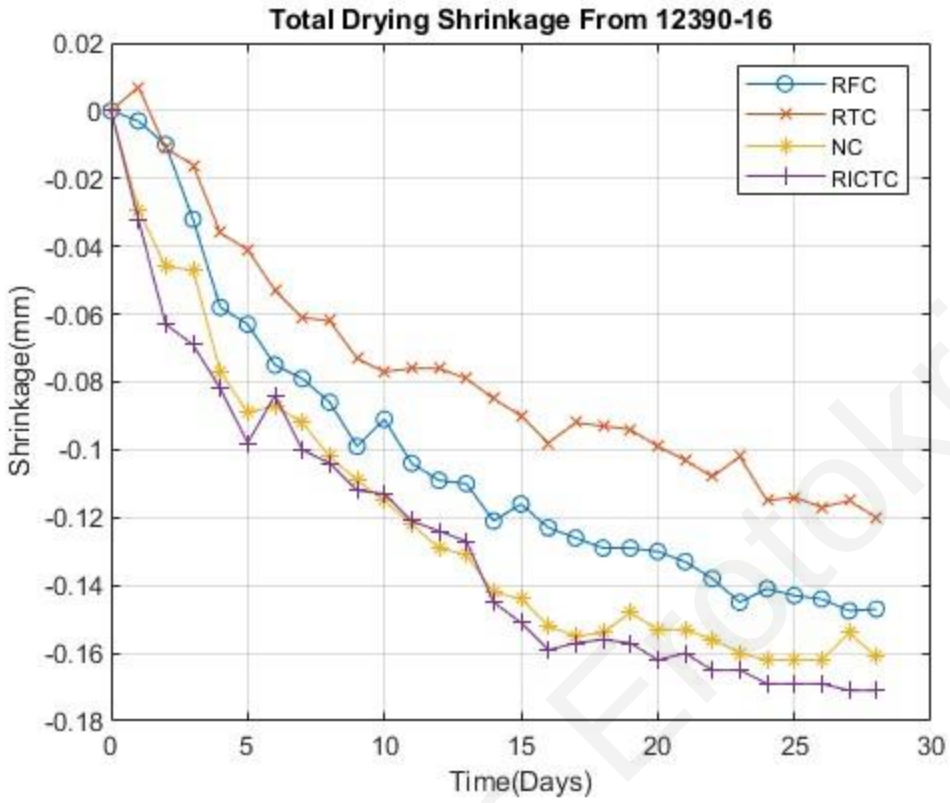

Figure 33 Total Drying Shrinkage of specimens versus time.

The test's standard also depicted the monitoring of mass loss (Figures 34-37). Based on these findings, the autogenous shrinkage specimens displaying the least mass loss were those that were internally cured (RICTC mixture). This can be attributed to the utilization of pre-soaked with water RCA, which provides anhydrous cement with the capability to access water compared to needing to absorb it from the surrounding environment. Additionally, this implies that the cement's impact on generating internal stress within the matrix is less pronounced compared to other specimens.

The behavior of the RTC specimens closely mirrors that of the No Curing (NC) specimens, with almost identical mass loss. This observation confirms the presence of anhydrous cement within the cement paste, intensifying the demand for water and consequently influencing the overall mixture.

In terms of Total shrinkage, the results demonstrate that during the initial five days, the rate of mass loss is higher in comparison to subsequent periods. Following this, the rate stabilizes, displaying an almost linear trend. This pattern might be attributed to the extensive hydration of a significant portion of the cement within the matrix during the initial phase. Subsequently, most of the mass loss can be attributed to the evaporation of water vapors from within the matrix.

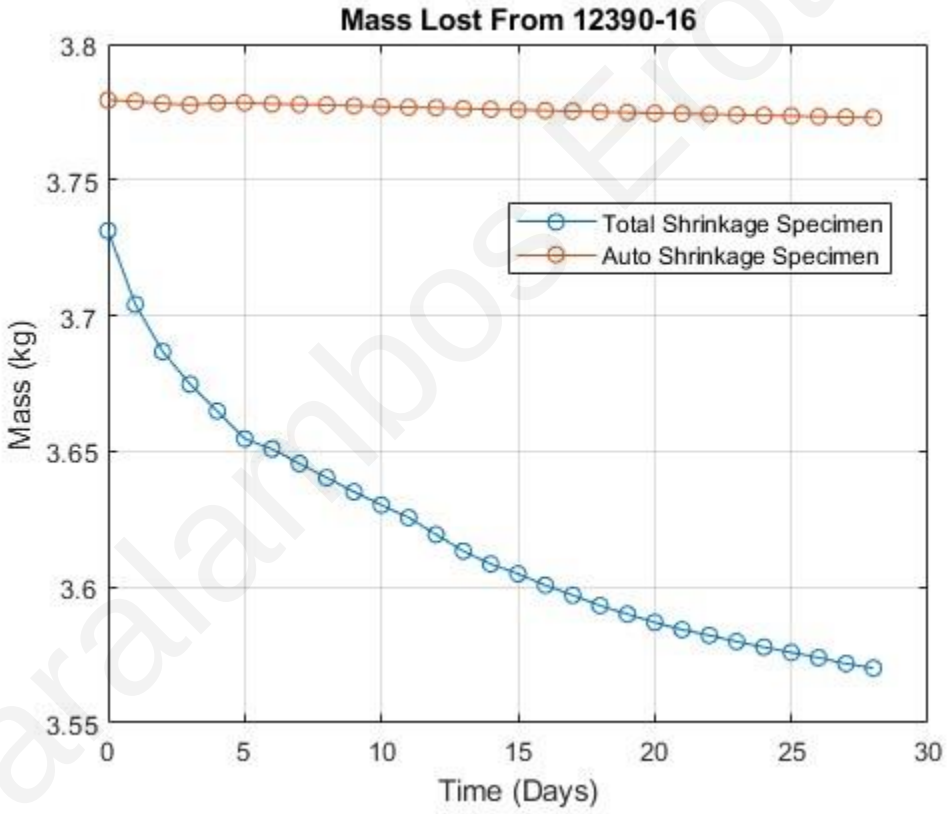

Figure 34: NC mixture total and autogenous mass loss versus time.

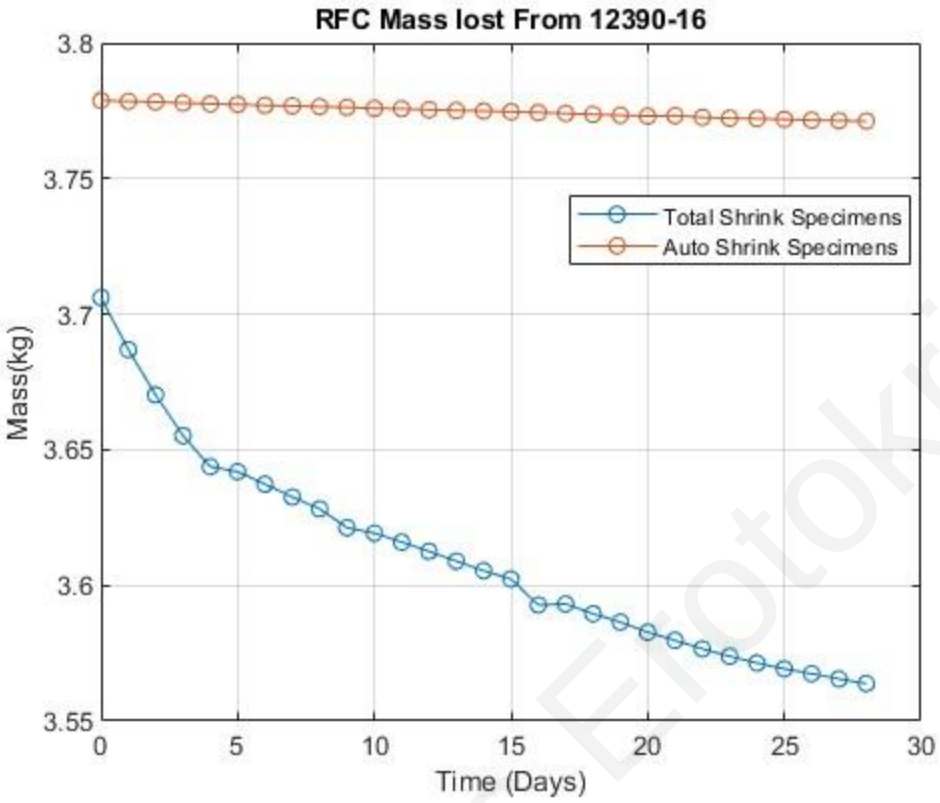

Figure 35: RFC mixture total and autogenous mass loss versus time.

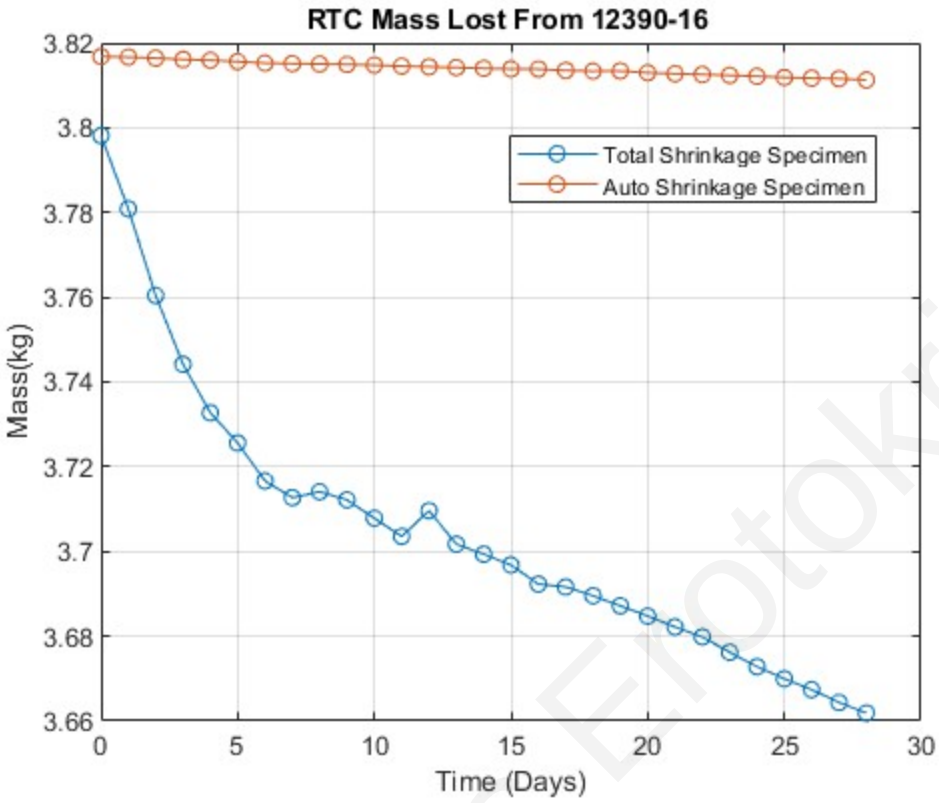

Figure 36: RTC mixture total and autogenous mass loss versus time.

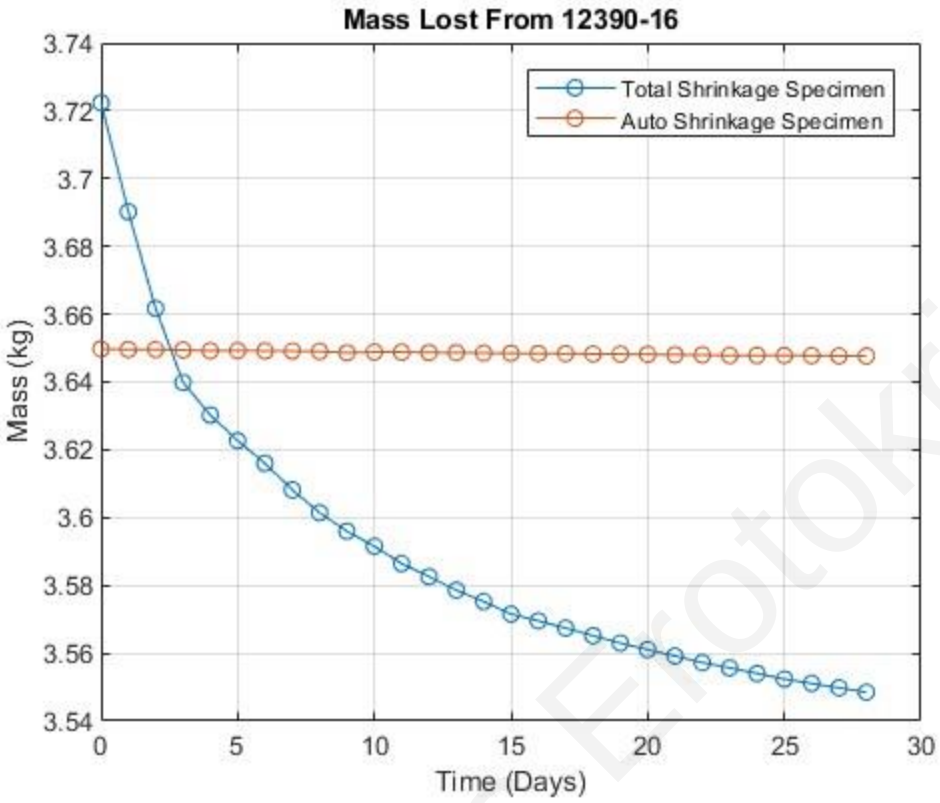

Figure 37: RTIC mixture total and autogenous mass loss versus time.

Figures 38 depicts the total mass loss from specimens. From the curves it is implied that RICTC total mass loss specimens lose water in a studier fashion than the rest specimens. They also reach equilibrium of mass loss faster. It is noticeable also that RTC specimens are losing water faster from the rest specimens until day 5 where the water loss gets studier. RFC specimens water loss reach a studier water loss pace after day 15, showing the bad influence of the hardened paste on the aggregates.

Figure 39 depicts the total autogenous mass loss from specimens. RTC and NC curve can be described almost similar. This is described from the fact that the water inside the ITZ is the one that is calculated. That water reacts with anhydrate cement leading to new products with smaller mass than the reactive ingredients. Since the aggregates are almost from identical material, the curves are almost the same. RFC specimens are also close to the RTC and NC curve. This is because the autogenous mass loss is not as impactfull as the total mass loss. Total mass loss takes water not bonded with cement from the external and internal water of concrete, while the autogenous is only from the inside. The internal water is in far less quantities than the external, which can be generated from the environment also. Thus, the reactions and furthermore the water loss is far less significant than the total mass loss.

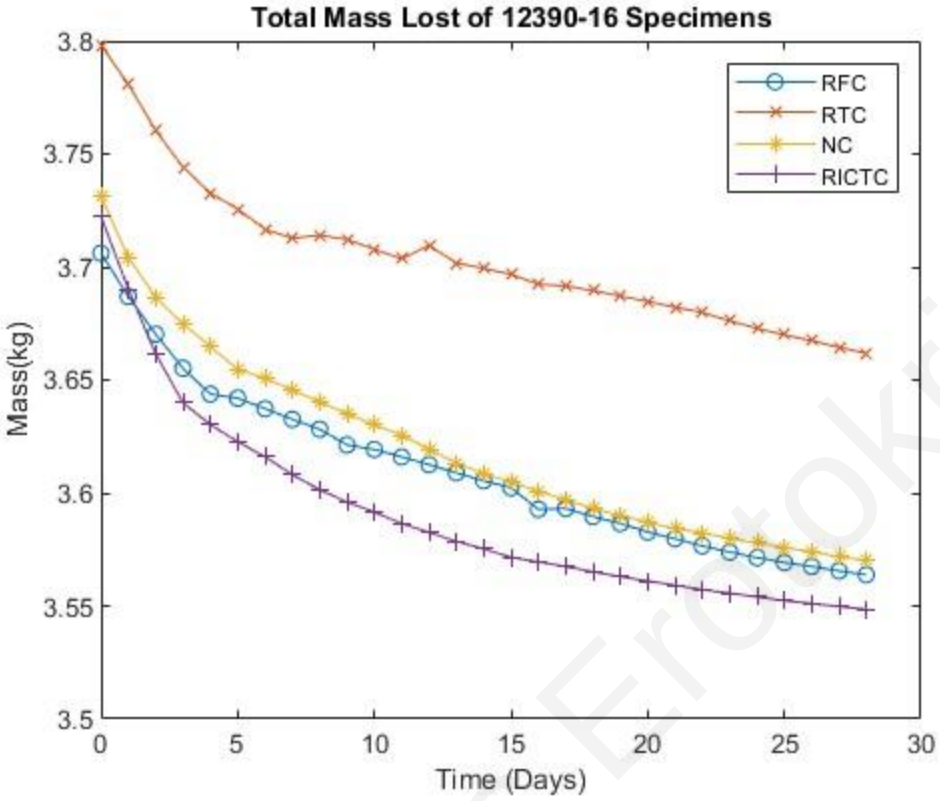

Figure 38 Total Mass Lost of specimens from 12390-16.

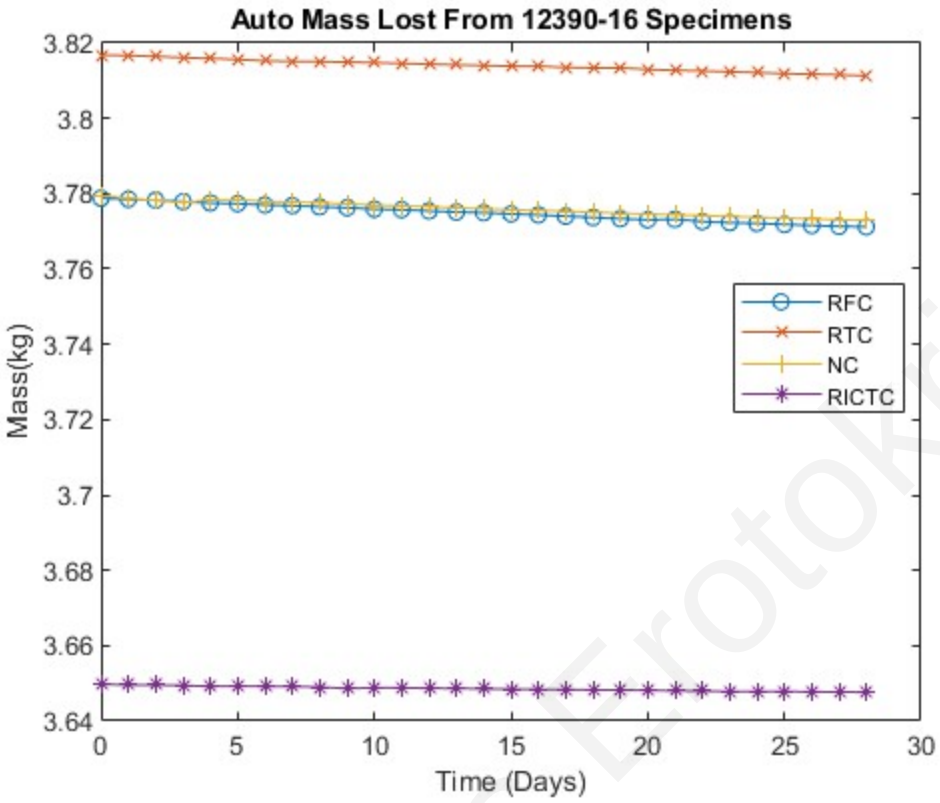

Figure 39 Total Autogenous mass lost of specimens from 12390-16.

5. Conclusions

The primary focus of this dissertation paper was to establish the importance of employing techniques to minimize the negative effects associated with the incorporation of Recycled Concrete Aggegates (RCA) in concrete mixtures. In general, with increasing percentages of RCA being used in replacement of the conventional aggregate content of a concrete mixture, there is a reduction in mechanical and physical properties. This research was conducted aiming to explore techniques that can improve the quality of RCA and therefore reduce the negative effects on concrete mix mechanical performance. Techniques such as water treatment and internal curing were employed and the effects on compressive strength, tensile strength, modulus of elasticity, porosity, sorpivity, autogenous and drying shrinkage properties were evaluated.

The conclusions drawn from the conducted tests are as follows:

- Pre-soaking RCA in water has been confirmed to reduce autogenous shrinkage.
- The influence of water curing extends to other mechanical and physical characteristics of concrete. Despite the fact that an increase in compressive strength, as anticipated from existing literature, was not conclusively established, parameters such as porosity, sorptivity, and modulus of elasticity showcased positive outcomes. The use of treated aggregates decreased the pores size of concrete and thus decreased porosity. In addition, this played as a factor to the increase of compressive & tensile strength and the increase of modulus of elasticity.
- The internal curing technique definitively demonstrated its potential in reducing the negative consequences associated with the incorporation of RCA in concrete mixtures, since the internally cured samples showed positives outcomes that are before mentioned, compared to the samples not internally cured internal curing helped the steady and continuous hydration of the anhydrate cement paste inside ITZ and that is a major factor in the before mentioned outcomes.
- Methods employed for the removal of hardened paste also demonstrated a positive impact on the mechanical and physical characteristics of the mixtures. To be precise, the use of treated aggregates decreased the porosity of concrete, which was a factor that helped the increase of compressive and tensile strength and modulus of elasticity. Shrinkage of concrete also showed to be positively affected by the treatment method, which made concrete lose less mass from autogenous shrinkage than its counterparts.
- Adhering to best practices and careful conditioning of concrete consistently is proven to lead to improvements in its mechanical characteristics, durability physical capabilities.

References

[1]: Gromicko, N., & Shepard, K. (2018). The History of Concrete - InterNACHI. *InterNACHI*.

[2]: Wikipedia. (2016). Concrete - Wikipedia, the free encyclopedia. In *Wikipedia, the free encyclopedia*.

[3]: Jamal, H. (2017). Applications and Uses of Aggregates. *Material Engineering*.

[4]: Mason, T. O. (2022). *Cement building material*. Encyclopedia Britannica.

[5]: Reddy Babu, G., Reddy, B. M., & Ramana, N. V. (n.d.). *QUALITY OF MIXING WATER IN CEMENT CONCRETE "A REVIEW."* www.sciencedirect.comwww.materialstoday.com/proceedings2214-7853©

[6]: Rob Banes & John Fifer, Aggregate Energy Consumption Guide Summary Report, table 3, 2009

[7]: Worldtada info, Energy consumption in Cyprus

[8]: Babor, D., Plian, D., & Judele, L. (2009). Environmental Impact of Concrete. *Buletinul Institutului Politehnic Din Lasi. Sectia Constructii, Arhitectura*, *55*(4).

[9]: Yang, G., Li, Q., Guo, Y., Liu, H., Zheng, S., & Chen, M. (2022). Study on the Mechanical Properties and Durability of Recycled Aggregate Concrete under the Internal Curing Condition. *Materials*, *15*(17). https://doi.org/10.3390/ma15175914

[10]: SUSTAINABILITY - FRANCE**,** Recycled aggregates: the circular economy supplying the construction sector, 2022

[11]: Tam, V. W. Y., Tam, C. M., & Le, K. N. (2007). Removal of cement mortar remains from recycled aggregate using pre-soaking approaches. *Resources, Conservation and Recycling*, *50*(1), 82–101. https://doi.org/10.1016/j.resconrec.2006.05.012

[12]: Dimitriou, G., Savva, P., & Petrou, M. F. (2018). Enhancing mechanical and durability properties of recycled aggregate concrete. *Construction and Building Materials*, *158*, 228–235. https://doi.org/10.1016/j.conbuildmat.2017.09.137

[13]: Velardo, P., Sáez del Bosque, I. F., Sánchez de Rojas, M. I., de Belie, N., & Medina, C. (2022). Durability of concrete bearing polymer-treated mixed recycled aggregate. *Construction and Building Materials*, *315*. https://doi.org/10.1016/j.conbuildmat.2021.125781

[14]: CYS EN 933-1:2012; Test for Geometrical Properties of Aggregates—Part 1: Determination of Particle Size Distribution—Sieving Method. CEN (European Committee for Standardization): Brussels, Belgium, 2012

[15]: Oikonomopoulou, K., Ioannou, S., Savva, P., Spanou, M., Nicolaides, D., & Petrou, M. F. (2022). Effect of Mechanically Treated Recycled Aggregates on the Long Term

Mechanical Properties and Durability of Concrete. *Materials*, *15*(8). https://doi.org/10.3390/ma15082871

[16]: CYS EN 933-2:2012, Tests for geometrical properties of aggregates – Part 2: Methods for reducing laboratory samples.

[17]: CYS EN 933-3; Tests for Geometrical Properties of Aggregates Part 3: Determination of Particle Shape–Flakiness Index. CEN: Brussels, Belgium, 2012.

[18]: CYS EN 933-4:2012, Tests for geometrical properties of aggregates – Part 4: Determination of particle shape – Shape index

[19]: ASTM C131/C131M-14; Standard Test Method for Resistance to Degradation of Small-Size Coarse Aggregate by Abrasion and Impact in the Los Angeles Machine. ASTM International: West Conshohocken, PA, USA, 2014; pp. 1–5.

[20]: CYS EN 1097-6:2013; Tests for Mechanical and Physical Properties of Aggregates—Part 6: Determination of Particle Density and Water Absorption. CEN (European Committee for Standardization): Brussels, Belgium, 2013.

[21]: BS 1881-125: 1986; Testing Concrete. The British Standards Institution: London, UK, 1986; pp. 1–14.

[22]: Jian, S. M., Wu, B., & Hu, N. (2021). Environmental impacts of three waste concrete recycling strategies for prefabricated components through comparative life cycle assessment. *Journal of Cleaner Production*, *328*. https://doi.org/10.1016/j.jclepro.2021.129463

[23]: Civil Engineering Portal, what is the significance of flakiness index and elongation index?

[24]: Pliya, P., Hajiloo, H., Romagnosi, S., Cree, D., Sarhat, S., & Green, M. F. (2021). The compressive behaviour of natural and recycled aggregate concrete during and after exposure to elevated temperatures. *Journal of Building Engineering*, *38*. https://doi.org/10.1016/j.jobe.2021.102214

[25]: Khoury, E., Cazacliu, B., & Remond, S. (2017). Impact of the initial moisture level and pre-wetting history of recycled concrete aggregates on their water absorption. *Materials and Structures/Materiaux et Constructions*, *50*(5). https://doi.org/10.1617/s11527-017-1093-8

[26]: Zaharieva, R., Buyle-Bodin, F., & Wirquin, E. (2004). Frost resistance of recycled aggregate concrete. *Cement and Concrete Research*, *34*(10), 1927–1932. https://doi.org/10.1016/j.cemconres.2004.02.025

[27]: Djerbi, A. (2018). Effect of recycled coarse aggregate on the new interfacial transition zone concrete. *Construction and Building Materials*, *190*, 1023–1033. https://doi.org/10.1016/j.conbuildmat.2018.09.180

[28]: Hasnaoui, A., Ghorbel, E., & Wardeh, G. (2021). Performance of metakaolin/slag-based geopolymer concrete made with recycled fine and coarse aggregates. *Journal of Building Engineering*, *42*. https://doi.org/10.1016/j.jobe.2021.102813

[29]: Yang, G., Li, Q., Guo, Y., Liu, H., Zheng, S., & Chen, M. (2022). Study on the Mechanical Properties and Durability of Recycled Aggregate Concrete under the Internal Curing Condition. *Materials*, *15*(17). https://doi.org/10.3390/ma15175914

[30]: Concrete Pavement Technology Center, N. (n.d.). *Impacts of Internal Curing on Concrete Properties Literature Review*. www.cptechcenter.org

[31]: CYS EN 12390-3:2009; Testing Hardened Concrete-Part 3: Compressive Strength of Test Specimens

[32]: CYS EN 12390-6:2009, Testing Hardened Concrete-Part 3: Splitting Tensile Strength of Test Specimens

[33]: EN 206-1, Concrete—Specification, Performance, Production and Conformity

[34]: Guy Woodford, Aggregate Business, The futures bright for the Cypriot aggregates sector, April 23, 2020

[35]: de Juan, M. S., & Gutiérrez, P. A. (2009). Study on the influence of attached mortar content on the properties of recycled concrete aggregate. *Construction and Building Materials*, *23*(2), 872–877. https://doi.org/10.1016/j.conbuildmat.2008.04.012

[36]: Savva, P., & Petrou, M. F. (2018). Highly absorptive normal weight aggregates for internal curing of concrete. *Construction and Building Materials*, *179*, 80–88. https://doi.org/10.1016/j.conbuildmat.2018.05.205

[37]: Bentz, D. P., & Geiker, M. R. (2002). *On the Mitigation of Early Age Cracking Dimensional Stability and Bond Performance of Grouted Connections View project DOLCEM-Dolomite calcined clay composite cement View project*. https://www.researchgate.net/publication/238603976

[38]: Hossain, A. B., & Weiss, J. (2004). Assessing residual stress development and stress relaxation in restrained concrete ring specimens. *Cement and Concrete Composites*, *26*(5), 531–540. https://doi.org/10.1016/S0958-9465(03)00069-6

[37]: Tritsch, N., Darwin, D., & Browning, J. (2005). *EVALUATING SHRINKAGE AND CRACKING BEHAVIOR OF CONCRETE USING RESTRAINED RING AND FREE SHRINKAGE TESTS*.

[39]: Gao, Y., Zhang, J., & Han, P. (2013). Determination of stress relaxation parameters of concrete in tension at early-age by ring test. *Construction and Building Materials*, *41*, 152–164. https://doi.org/10.1016/j.conbuildmat.2012.12.004

[40]: Choi, H., Lim, M., Kitagaki, R., Noguchi, T., & Kim, G. (2015). Restrained shrinkage behavior of expansive mortar at early ages. *Construction and Building Materials*, *84*, 468–476. https://doi.org/10.1016/j.conbuildmat.2015.03.075

[41]: Rong, H., Dong, W., Yuan, W., & Zhou, X. (2021). An improved ring test to assess cracking resistance of concrete under restrained shrinkage. *Theoretical and Applied Fracture Mechanics*, *113*. https://doi.org/10.1016/j.tafmec.2021.102976

[42]: Mao, J., Liang, N., Liu, X., Zhong, Z., & Zhou, C. (2023). Investigation on early-age cracking resistance of basalt-polypropylene fiber reinforced concrete in restrained ring tests. *Journal of Building Engineering*, *70*. https://doi.org/10.1016/j.jobe.2023.106155

[43]: CYS EN 12390-16:2009, Testing Hardened Concrete-Part 16: Determination of the shrinkage of concrete.

[44]: CYS EN 12390-13:2009, Testing Hardened Concrete-Part 13: Determination of secant modulus of elasticity of concrete.

[45]: Ioannis Ioannou, CEE 534, Lecture 4, Water absorption, University of Cyprus, 2023

[46]: Jamkar, S. S., & Rao, C. B. K. (2004). Index of Aggregate Particle Shape and Texture of coarse aggregate as a parameter for concrete mix proportioning. *Cement and Concrete Research*, *34*(11), 2021–2027. https://doi.org/10.1016/j.cemconres.2004.03.010

[47]: CYS EN 12390-7:2009, Testing Hardened Concrete-Part 7: Density of hardened concrete.

[48]: *Αθανάσιος Χ. Τριανταφύλλου Καθηγητής Πανεπιστημίου Πατρών Τμήμα Πολιτικών Μηχανικών Εργαστήριο Μηχανικής & Τεχνολογίας Υλικών ΔΟΜΙΚΑ ΥΛΙΚΑ ΠΑΤΡΑ 2005 7η Έκδοση*. (n.d.). www.sml.civil.upatras.gr

[49]: Pericles A. Savva, Department of Civil and Environmental Engineering, UCY, A Dissertation Submitted to the University of Cyprus in Partial Fulfillment of the Requirements for the Degree of Doctor of Philosophy, Internal Curing of Concrete Using Highly Absorptive Normal Weight Aggregates, June 2018